NANYANG TECHNOLOGICAL UNIVERSITY

DEVELOPMENT OF SMALL MOLECULE PROBE FOR SCREENING OF BACTERIAL RESISTANT ENZYME AND THEIR BIOMEDICAL APPLICATIONS

DEVELOPMENT OF SMALL MOLECULE PROBE FOR SCREENING OF BACTERIAL RESISTANT ENZYME AND THEIR BIOMEDICAL APPLICATIONS

CHAN HUI LING

CHAN HUI LING

SCHOOL OF PHYSICAL AND MATHEMATICAL SCIENCES

2018

2018

DEVELOPMENT OF SMALL MOLECULE PROBE FOR SCREENING OF BACTERIAL RESISTANT ENZYME AND THEIR BIOMEDICAL APPLICATIONS

CHAN HUI LING

CHAN HUI LING

School of Physical and Mathematical Sciences

A thesis submitted to the Nanyang Technological University
in partial fulfilment of the requirement for the degree of
Master of Science

2018

ACKNOWLEDGEMENTS

I would like to thank Assoc. Prof. Xing Bengang for his guidance during my M.Sc. research.

I am thankful to Junxin and other group members for their support and assistance during my period of research.

I would like to express my gratitude towards Prof. Chiba Shunsuke for his approval of his laboratory usage for the synthetic work, which greatly facilitated this research.

I am also extremely thankful towards Ciputra, Derek, Sherman, Hiro, and others for their constant guidance and support from my undergraduate to graduate period of studies.

I would like to thank Jin Yong for his contributions during his final year project, to the work presented in this thesis.

I would like to express my appreciation to the staffs from the Division of Chemistry and Biological Chemistry (CBC), Ee Ling and Wen Wei for their assistance with instrument trainings/usages; Janice, Si Yun, and Yean Chin for their assistance in graduate studies matters.

I would like to express my gratitude to Nanyang Technological University for the financial support during the original Ph.D. candidature, in the form of Nanyang Research Scholarship. I would also like to thank CBC for giving me the opportunity to attend the 2nd International Biophotonics Conference, Singapore.

Last but not least, I would like to thank my daddy and mummy for their support in my decisions regarding further studies. I am also extremely grateful to my friends, Gillian, Wei Ting, Wei Li, and others for their constant support and encouragement.

TABLE OF CONTENT

Abstract		iii
Publications		iv
Part I		
Chapter I	General Introduction	
1.1	Bacterial Cell Structure	1
1.2	β-lactam Antibiotics	4
1.3	β-lactamase Enzymes and its Classifications	10
1.4	Recent Developments in Small Molecular Probe Imaging of β-lactamase Activities	16
1.5	Gaps and Proposed Work	21
Part II		
Chapter II	Unique Fluorescent Imaging Probe for Bacterial Surface Localization and Resistant Enzyme Imaging	
2.1	Introduction	23
2.2	Recent Studies on Lipid for Cell Membrane Targeting	24
2.3	Reporter Molecule Design	27
2.4	Results and Discussion	28
2.5	Conclusion	42
Part III		
Chapter III	Experimental Section	
3.1	General Informations	43
3.2	General Procedures	44
3.3	References	53

ABSTRACT

The work in this thesis has been aimed towards development of a small molecular probe for the screening of bacterial resistant enzymes. This thesis is divided into three main parts:

- Part I incorporates an introduction to gram positive and negative bacteria and its cell structure, β-lactam antibiotics with a brief insight into various core structure that drugs commonly consist of, β-lactamase enzyme mechanisms and the classifications, recent development in the use of small molecular probe for β-lactamase activities monitoring and imaging, as well as the current gaps and proposed work.
- Part II disclosed on a covalent labelling approach towards imaging AmpC β-lactamase activity on bacteria cell wall.
- Part III encloses the experimental data and references.

PUBLICATIONS

1. **Chan, H. L.**,[†] Lyu, L.,[†] Aw, J.,[†] Zhang, W.,[†¶] Li, J.,[¶] Yang, H.-H.,[¶] Hayashi, H,[†] Chiba, S.,[†] Xing, B.,*[†¶] *ACS Chem. Biol*. **2018,** Just Accepted Manuscript DOI: 10.1021/acschembio.8b00172

Chapter I. General Introduction

1.1 Bacterial Cell Structure

Bacteria, one of the oldest living organisms on Earth, are unicellular prokaryotic microorganisms that play an essential function in regulating processes in the ecosystem as well as in living organisms.[1-2] In the ecosystem, bacteria play a significant role through cycling of carbon, nitrogen, and sulfur based nutrients; while in living organisms, although some bacteria cause serious diseases, numerous aid regulation of daily activities. To give an example, *Escherichia coli* in human large intestine synthesize vitamin K_2, important for properly facilitated blood coagulation.

Bacteria can usually be broadly categorized into the gram positive and gram negative (Figure 1).[3-4] The two bacterial types with different cell wall structures, display distinctively different cell envelope properties and abilities. Gram staining is a simple technique widely employed to differentiate both types of bacteria. Firstly, bacteria are stained with a crystal violet dye, followed by excess dye removal. Gram positive bacteria are able to retain the dye due to their thicker peptidoglycan layer thus appearing violet; whereas gram negative bacteria with a thinner peptidoglycan will have the dye displaced. Subsequent addition of a safranin counterstain will generate pink stained gram negative bacteria, while gram positive bacteria that had been stained a strong dark violet, will have minimum observatory changes.

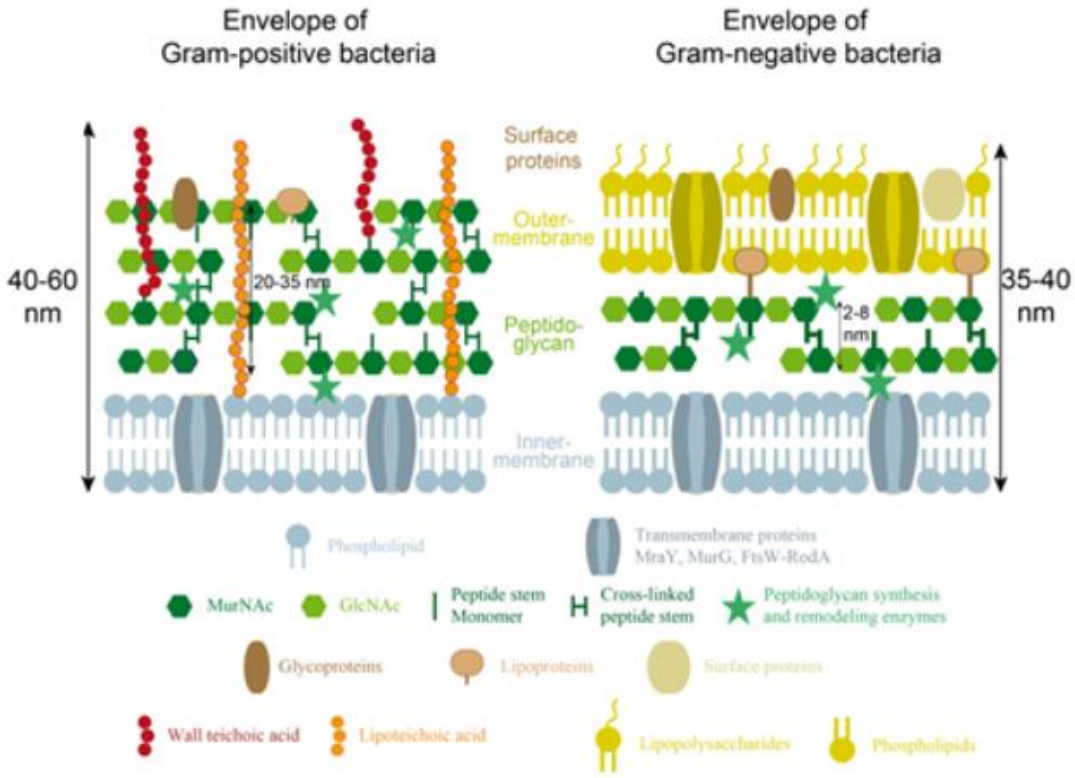

Figure 1. Bacterial envelope of gram positive and gram negative bacteria[5]

Gram positive bacterial cell wall consists of a thick layer of peptidoglycan followed by the cytoplasmic membrane. On the other hand, gram negative bacteria express an additional outer membrane that envelopes a thin layer of peptidoglycan, followed by the cytoplasmic membrane. The essential presence of the outer membrane in gram negative bacteria act as a selective partition to lower susceptibility of the microorganism towards harmful molecules.[6-7] This resultant effect is partially due to the decreased permeabilization of chemical substances, while enabling regular nutrients influx for robust bacterial survival.

The distinct gram negative bacteria macromolecular assembly, the outer membrane comprises of the asymmetric hydrophobic lipid bilayer. The layer vastly constitutes of an inner phospholipids leaflet, an outer lipopolysaccharides leaflet that composes of the hydrophobic lipid A attached to the hydrophilic linear polysaccharides of core oligosaccharides and O-antigens, porins, and lipoproteins.

The lipoproteins are anchored onto the outer membrane layer and bonded covalently to the peptidoglycan.[8-9] Its strategical situation has resulted in the observation of lipoproteins playing a role in the outer membrane integrity stabilization, and renders interaction between the outer membrane and peptidoglycan. In addition, the bacterial lipid bilayer has an exceptional hydrophobicity due to the situated outer lipid A moieties which is capable of conjugating six fatty acid chains as compared to two chains in a typical phospholipid bilayer. The lipid bilayer thus induces a stronger lateral interaction between the lipopolysaccharide molecules while lowering the fluidity, resulting in the observed molecular selectivity of the outer membrane.

In the bacterial species, the peptidoglycan structural framework is a crucial feature of the bacterial cell wall.[10] Its presence is critical for for bacterial division, maintaining bacterial cell shape, preventing bacterial cell lysis from the high osmotic pressures across the bacterial internal and the external environment, as well as to provide a stable scaffold for anchoring of the transmembrane complexes and the integrated membrane proteins.[11] Gram negative bacteria have a thin peptidoglycan of approximately 2-7 nm, while gram positive bacterial peptidoglycan make up the main constituent of 20-35 nm.[12-14] The peptidoglycan layer consists of alternating monosaccharide units of *N*-acetyl glucosaminem (GlcNAc) conjugated to *N*-acetyl muramic (MurNAc) through intramolecular ether linkage at the C4 and C1 position respectively, with each MurNAc sugar connected to a pentapeptide chain of L-Alanine-D-Glutamate-*meso*-diaminopimelic acid-D-Alanyl-D-Alanine (L-Ala-D-Glu-*m*-Dap-D-Ala-D-Ala). The pentapeptide chain units can differ considerably between different bacterial species. The other components integrated into the gram positive bacterial peptidoglycan are teichoic acids, lipoteichoic acids, and proteins.

The mesh-like sheets of peptidoglycan are formed by cross-linking disaccharide sugar monomers at the fourth positioned D-Ala on one pentapeptide stem to the third positioned *m*-Dap on the other pentapeptide by a D,D-transpeptidase enzyme, forming the traditional 4→3 D-Ala-*m*-Dap linkage (Scheme 1).[15] The D,D-transpeptidase, commonly known as the penicillin-binding protein (PBP), accommodates a serine amino acid in its active site and connects majority of the final peptidoglycan synthesis in most bacteria. This cross-linking mechanism can differ in numerous ways, hence resulting in wide connection varieties for varied macrostructures in different bacterial species, depending on the peptidoglycan variants utilized for synthesis.

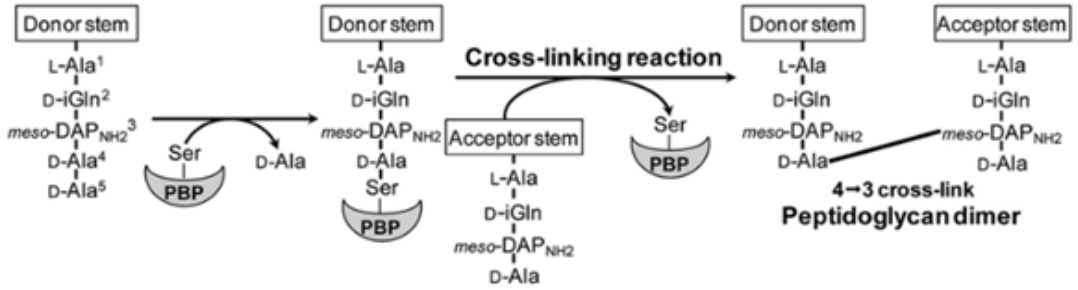

Scheme 1. PG synthesis by PBP[15]

1.2 β-lactam Antibiotics

Due to the peptidoglycan importance for bacterial survival and growth as discussed in chapter 1.1, interference with peptidoglycan synthesis has been a target of many antibacterial agents to block the cross-linking process of the pentapeptide bridges, therefore inducing bacterial lysis from the weakened cell wall. One example of the antibacterial agent is the β-lactam antibiotic,[16] which targets the PBP irreversibly to inhibit its activity.

β-lactam drugs are a class of broad-spectrum antibiotics composed of the nitrogen-containing β-lactam ring in the molecular core structure, the key to the antibiotic mode of action (Figure 2). β-lactam antibiotics are remarkably recognized

by the PBP due to the hydrolyzed ring opened structure ability to mimic D-ala-D-ala backbone, found at the fourth and fifth position of the pentapeptide (Figure 2 and Scheme 2).[17-20] Crucially in β-lactam ring, the reactive CO-N bond lies in a similar structural conformation as the D-ala-D-ala moiety CO-N bond. The β-lactam drug therefore works similarly through competitive binding to the PBP active pocket serine amino acid. This prevents PBP coupling to D-ala-D-ala, thereby inducing bacterial death through the inhibition of a stable bacteria cell wall formation.

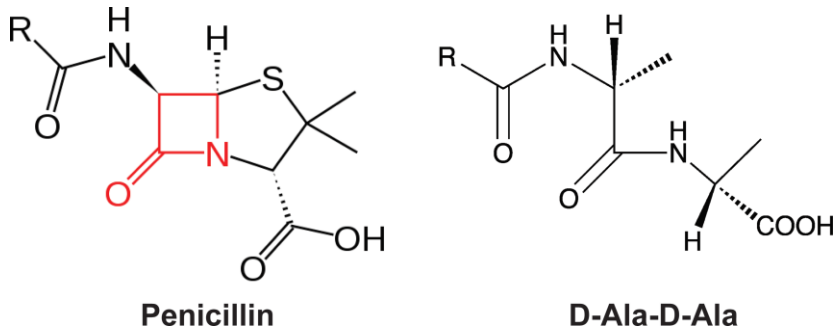

Figure 2. Structural comparison of penicillin with bacterial D-ala-D-ala[18]

The amide in the β-lactam is unusually reactive towards hydrolysis due to the four-membered ring strain, as well as the conformational arrangement that prevents interaction of the nitrogen lone pair with the carbonyl. Furthermore, it has been shown in both functional and structural studies that the β-lactamase enzyme which breaks down β-lactam antibiotics (discussed in chapter 1.3), contains an oxyanion hole at the enzymatic active site which stabilizes the tetrahedral intermediate.[21-23] This reduces the transitional energy state and further promotes β-lactam ring shift towards the ring opened conformation.

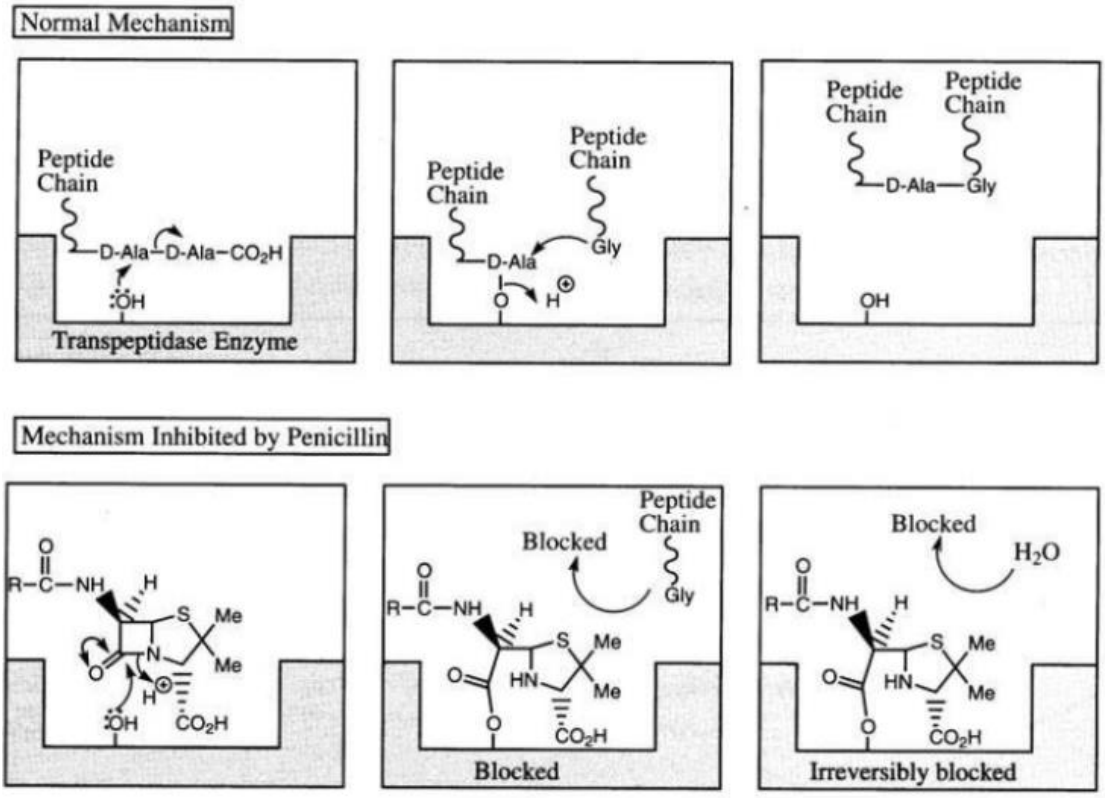

Scheme 2. PBP cross-linking function and its inhibition[24]

Natural β-lactam antibiotics are found in some fungus species and its usage for infection treatments have been dated back to ancient times.[25] However, the main breakthrough in the field of medicine was in the year 1928 when Sir Alexander Fleming, a Scottish biologist, discovered the β-lactam substance penicillin from the fungus *Penicillium notatum*.[26] This revolutionized treatments in combatting infections years later, such as the deadly tuberculosis caused by the bacteria *Mycobacterium tuberculosis*.[16, 27] In fact, Sir Alexander Fleming was not the first scientist to observe an organism's ability to secrete substances that interfere with the growth of another. Various other earlier scientists to note this correlation include John Parkington,[28-29] Sir John Scott Burdon-Sanderson,[30] William Roberts,[31] Joseph Lister,[32] John Tyndall,[33] Louis Pasteur, and Jules Francois Joubert.[17, 34] Besides fungus, many antibacterial compounds were isolated from bacterial species which further expanded the β-lactam antibacterial potency spectrum. Most notably, the isolation of

cephalosporin from *Cephalosporium acremonium*,[35-36] monobactam from *Chromobacterium violaceum*,[37] and carbapenem from *Streptomyces cattleya*,[38] contributed critically to the medicinal field (Figure 3).

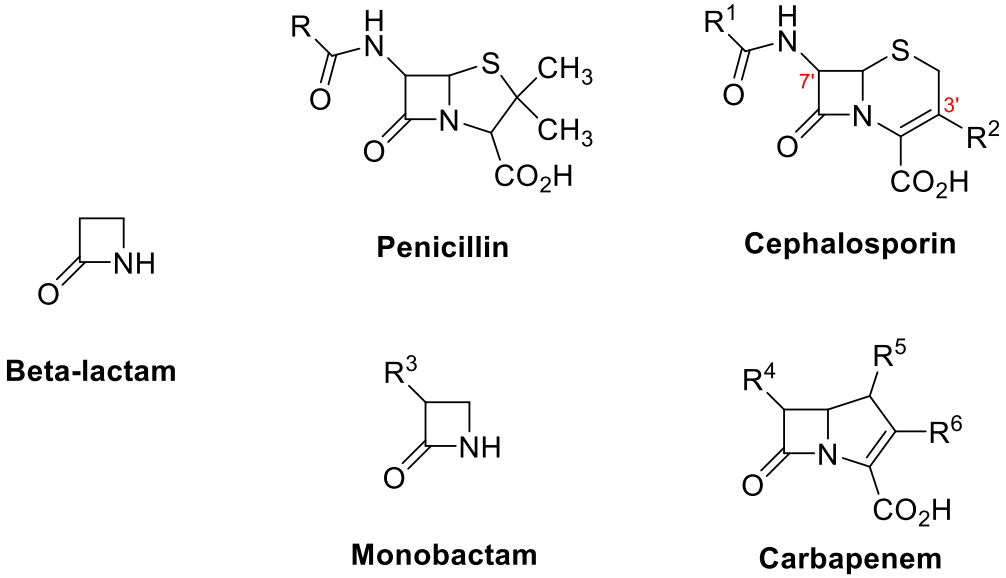

Figure 3. Core structure of different type of β-lactam drugs

In the market today, an extensive variety of β-lactam antibiotics are retailed. The β-lactam drugs are extensively utilized due to the superior effectiveness in treatment of bacterial infections. Currently, various forms of intake, oral, intravenous and intramuscular, are made available.[39]

Dosage of β-lactam drug to administer for efficient treatment is based on the ability to achieve a plasma concentration exceeding the minimum inhibitory concentration (MIC) of the targeted bacteria, through dosage frequency and for a substantial time period in order for the drug to work optimally.[40-41] MIC refers to the lowest concentration of a substance required to inhibit bacterial growth. A lower MIC value indicates the effectiveness of the drug towards a specific bacterium since a low concentration is needed to significantly hinder the bacterial survival. Importantly, different bacteria can have varied MIC susceptibility for the same drug. β-lactams reaches the peak efficacy at five-folds of MIC, with no further antibacterial effect

above that concentration.[42] Moreover, bactericidal activity of β-lactam molecules are determined by the exposure duration instead of the degree above the MIC value. In addition, many β-lactam agents would be optimally dosed if given over a longer period of time since β-lactams have a short half-life.[39] Half-life is the time duration needed for the substance to reach half of its original concentration. A small half-life value indicates a need for frequent dosing which could be a primary result of faster metabolism or better excretion function of the body system to the drug. The smaller half-life value not only suggests reduction in the antibacterial effect time period, but also of any side effect the drug may induce.

β-lactam based drugs are commonly classified according to their core structure into the penicillin, cephalosporin, monobactam, and carbapenem subclasses, excluding β-lactam based inhibitors, which will be briefly introduced below.[16]

1.2.1 Penicillin

Penicillin is a group of antibiotics with a β-lactam ring connected to a thiazolidine core that are among the earliest prescribed to target various gram positive bacterial infections.[43] However, its extensive utilization in the early years resulted in many bacterial species developing resistance to the natural penicillin. Despite the resilience, penicillin evolution extended its diversity to those of narrow, broad and extended spectrum, and demonstrated efficacy towards gram positive and gram negative bacteria.[44] The semi-synthetic variation of penicillin has a greater resistance towards penicillinases, the enzyme responsible for the degradation of many natural penicillin. Today, penicillin remains one of the most important antibiotic widely used.

1.2.2 Cephalosporin

Cephalosporin is another group of antibiotics with the β-lactam ring conjugated to a 3,6-dihydro-2*H*-1,3-thiazine.[45] Its action mechanism is the same as the other β-lactam drugs, but with less susceptibility towards β-lactamase enzyme hydrolysis.[46] The additional stability and broad activity spectrum allows effective treatment of various infections, resulting in emergence of multidrug-resistance bacteria from its extended usage. Cephalosporin contains a 3'-positioned substituent that contributes minimally towards antibacterial activity, and is readily eliminated upon enzyme activity (Figure 3). The key position is at the cephalosporin 7'-position, which influences the antibacterial activity of the drug as well as affect the binding of β-lactamase enzymes due to its insertion into the active binding pocket. Cephalosporins are often categorized into different generations based on their overall antibacterial properties.[47-49] The first generation has good activity towards gram positive bacteria with limited effectiveness for gram negative bacteria. The second generation exhibits an improvement in gram negative bacteria depletion, however with lesser effectivity for the gram positive bacteria. The third generation cephalosporin shows an increased activity towards gram negative bacteria. Importantly, the drugs target well to β-lactamase production. However, the third generation drugs are generally less efficient towards gram positive bacteria than the second generation. The fourth generation are similar to the third generation in targeting gram negative bacteria with more stability towards β-lactamases, particularly towards class C β-lactamase enzymes. Importantly, the fourth generation zwitterion antibiotics have enhanced activity towards gram positive bacteria, thus making it a superior broad spectrum antibiotic.

1.2.3 Monobactam

Monobactam contains only the β-lactam ring, and unlike other β-lactams, monobactams are only effective against gram negative bacteria.[50] Monobactams are relatively stable towards β-lactamases. Despite its stability, there is an emergence of widespread resistance towards monobactam due to its frequent usage. Currently, the only available monobactam antibiotic is the aztreonam with a narrow spectrum activity.[51]

1.2.4 Carbapenem

Carbapenem with β-lactam coupled 2,3-dihydro-1*H*-pyrrole ring, often used as a reliable "antibiotic of last resort", has the broadest activity spectrum as well as potency in elimination of the gram positive and gram negative bacteria. Carbapenem exhibits stability to wide varieties of β-lactamase enzymes.[52] Many multidrug-resistant hospital-acquired bacteria are also sensitive to its presence. Similarly to the other antibiotics, carbapenem effectiveness resulted in the antibiotic's overuse, therefore resistance bacterial species have increased over the years.[53] The resistance poses a highly critical problem as there are few option towards treatment of carbapenem-resistance bacteria.

1.3 β-lactamase Enzymes and its Classifications

With the antibiotic discovery and development, its usage has led to a significant decrease in death from bacterial infections. However, its extensive consumption had accelerated bacteria transformation in acquiring complicated resistant mechanisms, which resulted in bacterial infections being harder to treat. One of the principle and efficient resistance mechanism bacteria developed is the secretion of periplasmic β-

lactamase enzymes to combat β-lactam antibiotics through hydrolysis of the drug thus deactivating its antibacterial properties, preventing PBP targeting.[54] Of the multiple modes of bacterial resistance, β-lactamase mechanisms have been intensively studied in great detail. Therefore, the individual characteristics of β-lactamases will be focused on and described below.

As an example, in the acylation step, class A β-lactamase (TEM-1) serine oxygen at the 70th position attack bicyclo[3.2.0]heptane β-lactam amide bond (Scheme 3).[55-56] This cleaves the bond to form an ester intermediate ES* with the β-lactam nitrogen reduced. Deacylation that follows utilizes a glutamate residue at the 166th position to hydrolyse the intermediate ES* ester bond, yielding the ring opened product along with the free TEM-1.

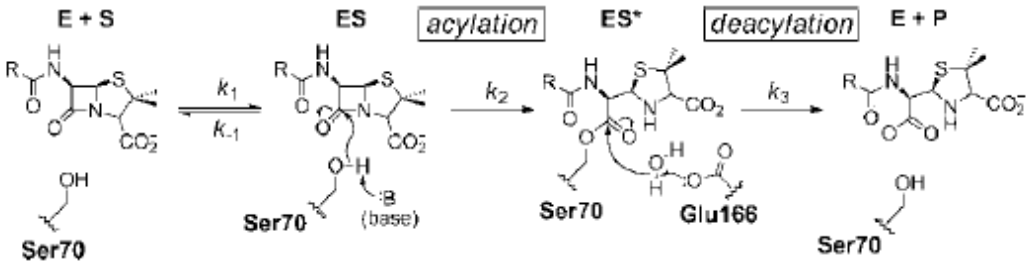

Scheme 3. TEM-1 hydrolysis mechanism of β-lactam

Bicyclo[4.2.0]oct-2-ene β-lactam on the other hand allows release of its 3'-positioned moiety through the same mechanism (Scheme 4).[55, 57] Serine oxygen at the binding pocket of the β-lactamase enzyme will first attack the β-lactam carbonyl. Following, electron shifts will eliminate the OR^{2}' anion. Subsequent hydrolysis releases the active β-lactamase and the inactive β-lactam. With the drug deactivated, bacteria species therefore become resistant to that form of antibiotic.

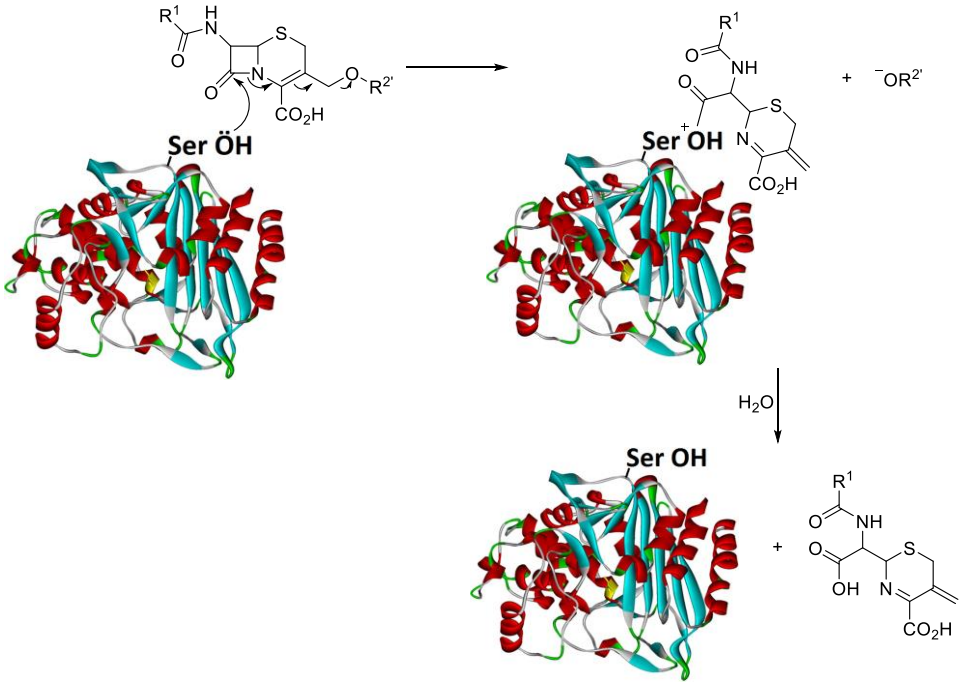

Scheme 4. Ring opening of 6 membered β-lactam by β-lactamase

Currently, there are two different methods to group the β-lactamase enzymes.[58] β-lactamases which are sorted based on Ambler classification, are organized into classes A, B, C, and D.[59] Each class correlates to the structural similarity of the β-lactamase amino acid sequences; whereby class A, C, and D contain a serine amino acid in its enzymatic pocket, whereas class B acts through a zinc(II) metal coordination.

1.3.1 Ambler Class A

Ambler class A β-lactamase exhibits the highest degree of diverse sequences, resulting in wider enzymatic properties as compared to the other subclasses.[60] Many are susceptible to the effect of clavulanic acid. Its enzyme type includes, but is not limited to the narrow-spectrum β-lactamases TEM and SHV that bind penicillins and some cephalosporins,[61] as well as the extended-spectrum β-lactamases (ESBLs) TEM, SHV, and CTX-M which target numerous β-lactam drugs,[62] and the clinically

important carbapenemases KPC, GES, IMI, and SME that target preferentially the carbapenem substrates.[63] With mutated class A β-lactamase as part of the ESBLs, the third and fourth generation cephalosporin as well as the monobactams can be readily inactivated unlike with the narrow-spectrum β-lactamases. More importantly, BlaC enzymes are responsible for the deadly tuberculosis diseases due to its high activity, resistance and survival mechanism.[64] One of the key attributes to inhibition of this class of β-lactamases with the exception of carbapenemases, is the decrease of the steric hindrance at R, R^1, R^3, and R^4 of the β-lactam antibiotics (Figure 3).[65-66] This decrease in bulkiness of the antibiotic ensures the successful accommodation of the drug side chain into the enzymatic active pocket, thereby leading to effectual blockage of the β-lactamase binding pocket.

1.3.2 Ambler Class B

Ambler class B metallo-β-lactamases (MBLs) involve participation of a mono- or di-Zn^{2+} coordinated to histidine, cysteine, and aspartic acid moieties at the active site (Scheme 5).[67] MBLs can be further divided into subclasses B1, B2, and B3, according to the homological primary amino acid sequences and the similar active mechanisms.[68] In addition, subclasses B1 and B2 are sequence homologs. The subclasses differ by the crucial Zn^{2+} ions binding motifs around the β-lactamase active pocket.[69] While subclasses B1 and B3 display the greatest activity with the participation of di-Zn^{2+} cation, subclass B2 preferably work as a mono-Zn^{2+} cation activation mechanism, with a decrease in activity when two Zn^{2+} binds to the activity site.[66] In MBLs, nucleophilic water cleave the β-lactam bond unlike with the serine based β-lactamases. In subclass B2, basic histidine deprotonates the water molecule which then reacts with the β-lactam amide bond, inactivating the antibiotic (Scheme

5A). Subsequent β-lactam nitrogen hydrolysis releases the hydrolyzed drug. The critical Zn^{2+} cation coordinating the three amino acids and the second water molecule react with the antibiotic carboxyl, allowing the tetrahedral intermediate after deacylation to be stabilized. In the case of subclasses B1 and B3, the first Zn^{2+} functions by decreasing the pK_a of a water molecule, generating the hydroxyl anion to cleave the amide bond, and the second Zn^{2+} functions to stabilize the tetrahedral intermediate (Scheme 5B). All of the MBLs are carbapenemases, therefore rendering most β-lactam antibiotics ineffective. Currently in the market, no inhibitor effective against MBLs are available, although inhibition can be achieved with metal chelating agents, for example, ethylenediaminetetraacetic acid (EDTA). However, EDTA has not been used in clinical tests due to its toxicity.

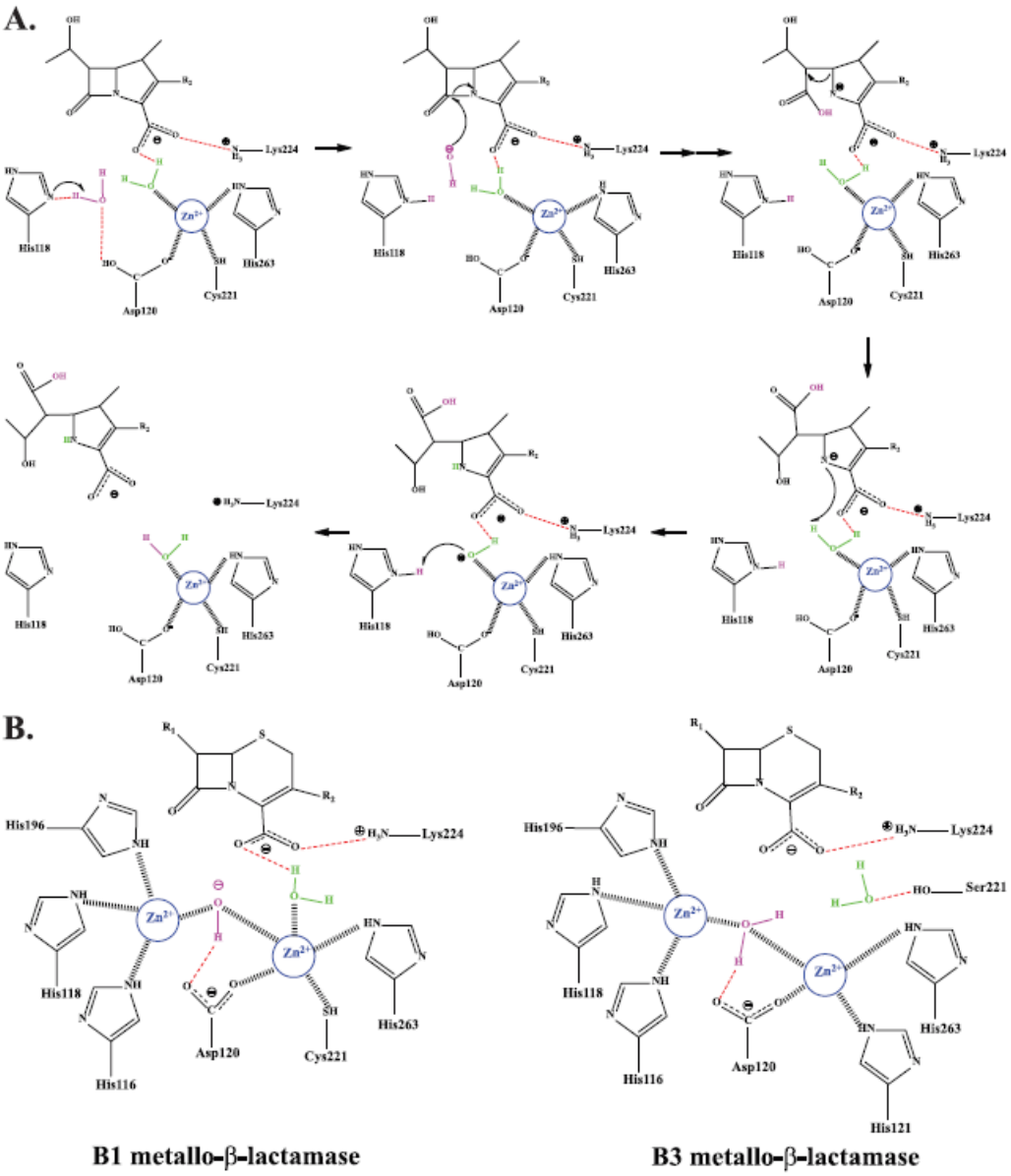

Scheme 5. A) Metallo-β-lactamase subclass B2 hydrolysis mechanism[66] B) Subclasses B1 and B3 di Zn^{2+} positioned for water activation

1.3.3 Ambler Class C

Ambler class C β-lactamases contain a serine amino acid in its enzymatic pocket.[70-74] They are active towards penicillin and cephalosporin, and are usually not carbapenemases, as most of the enzymes have weak or no activity towards carbapenem; although a rare amount has been found to confer resistance, prominently

the CMY-10 enzyme.[66] In this class of β-lactamases, ampC enzymes are found chromosomally or plasmid-mediated in bacteria, and are clinically important cephalosporinases that break down a broad range of β-lactam antibiotics.[75-76] AmpC however can be successfully treated with carbapenem.[77-78] Distinctively, class C β-lactamases have a larger binding pocket as compared to its counterpart class A β-lactamases.[65] This difference in pocket size allows specificity and selectivity towards class C β-lactamases through bulky side group employment. Typically, class C enzymes are resistant to various β-lactam inhibitors.

1.3.4 Ambler Class D

Ambler class D β-lactamases, similar to class C β-lactamases, are structural homolog with no sequence homology to class A β-lactamases.[51, 79] They have a high activity towards carbapenem-based antibiotic besides targeting penicillin and cephalosporin, making the acquisition or production of class D β-lactamases by bacteria deadly. Class D enzymes are commonly referred to as oxacillinases (OXA) due to its high activity towards oxacillin. Most ambler class D enzymes are poorly or unable to be inhibited by β-lactam inhibitors. With mutations, class D β-lactamases can become ESBLs, making its treatment even tougher.

1.4 Recent Developments in Small Molecular Probe Imaging of β-lactamase Activities

In recent years, studies have been conducted to enable a better understanding and to explore for a simpler detection and observation of β-lactamase activities. Among the investigations, small molecular probe development for the *in vitro* imaging of live bacteria with β-lactamase enzymes expression have been widely

explored. Its utilization has received huge interest in advanced technology due to the ease in the chemical properties modification, and its small size relative to fluorescent proteins and nanoparticles, which might reduce disruptiveness to living systems.[80] In addition, microscopy techniques have made drastic improvements to give accurate and reliable results in a short amount of time, hence making it one of most employed methods in clinical and pre-clinical early diagnosis tests.[81] Today, imaging technique development allows it to be utilized as one of the most robust tool in monitoring and analysis of pathogen-host interaction.

Various techniques for off-on fluorescent imaging have been developed and are widely utilized like fluorescence resonance energy transfer (FRET), photoinduced electron transfer (PeT), and intramolecular charge transfer (ICT) (Scheme 6).[82-84] FRET has been utilized most commonly among the three techniques due to its universal applications, advantage in the design flexibility, as well as having a wider choice of fluorophores ranging from molecules to particles. Its design flexibility includes constructable distance of 2-10 nm as compared to ICT and PeT narrower range, therefore enabling wider design experimentation to achieve the ideal molecular model. Larger varieties in fluorescence detection methods of FRET also make it an attractive option, for example intensity and polarity change. With all the advantages provided by utilizing FRET, it allows less limitation to the design model, and therefore more varieties of molecular probes designable for a wider purpose.

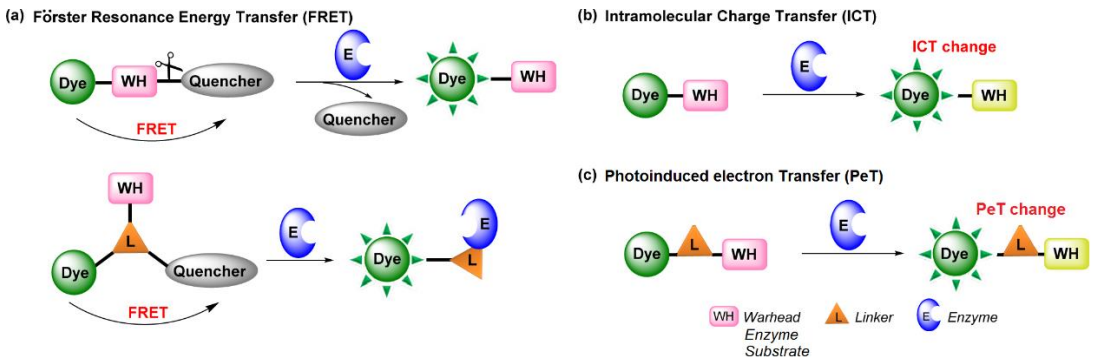

Scheme 6. Fluorescent imaging techniques[82]

In 2013, Xing's group came out with a covalent localization probe for specific labelling and imaging of β-lactam resistant bacteria (Scheme 7).[85] They utilized cephalosporin core structure with a sulfoxide for improved stability. The core β-lactam ring was conjugated with *para*-hydroxybenzylic ester bearing FRET pair. Exposure of TEM-1 to the probe induced cleavage of the *para*-hydroxybenzylic ester, which then underwent 1,6-elimination to release the quencher and generate the fluoresce quinone methide intermediate. Nucleophiles on resistant bacterial cell membrane then attacked the intermediate, resulting in the fluorescence imaging of localized covalent bacterial labelling.

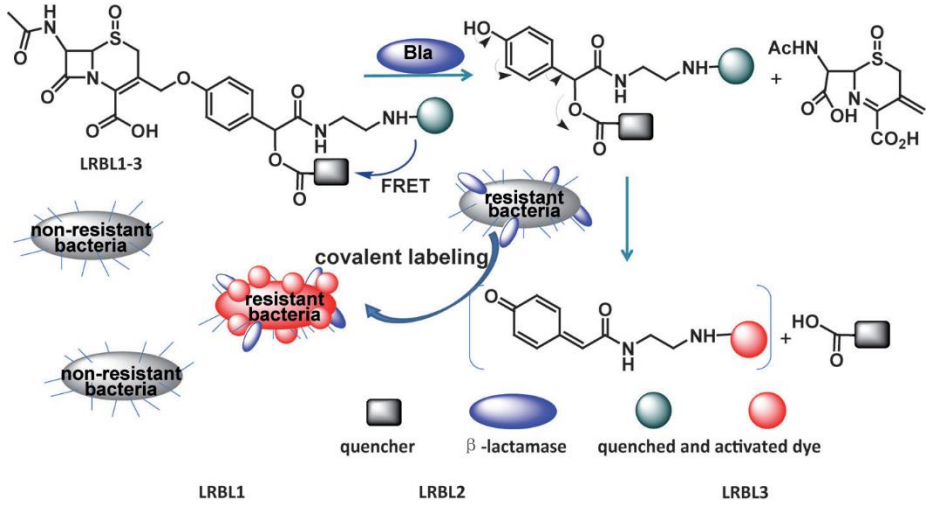

Scheme 7. Covalent labelling of TEM–1 resistant bacteria

Ma and coworkers in 2014 developed a highly sensitive small molecular probe for efficient β-lactamase quantification through fluorescence response intensity (Scheme 8).[86] The cephalosporin 3rd position was coupled with a hemicyanine fluorophore which showed weak fluorescence due to the hemicyanine hydroxyl moiety alkylation. Under the presence of β-lactamase, the cephalosporin β-lactam ring was readily cleaved, thereby releasing the hemicyanine fluorophore moiety and generated a significant fluorescence enhancement in the near-infrared wavelength.

The sensitivity of the fluorescence probe was shown by imaging of three *Staphylococcus aureus* bacteria with varied β-lactamases expressed levels. The resulting images revealed distinctively different expression levels in the three strains of bacteria.

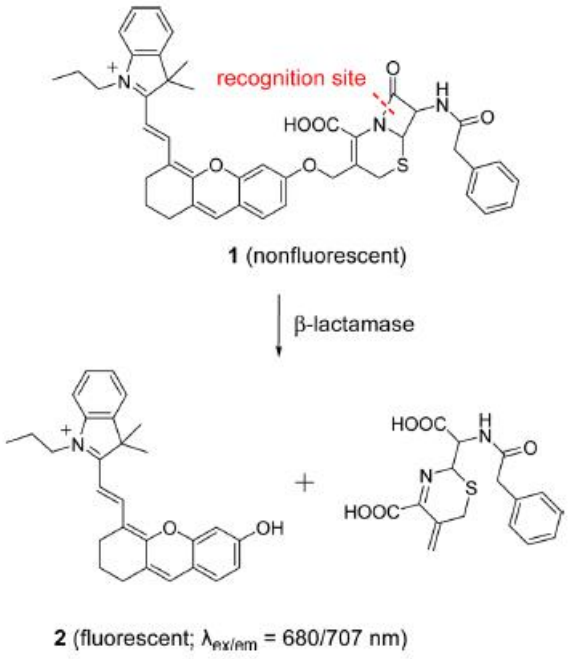

Scheme 8. Hemicyanine fluorophore release generating fluorescent

Xie reported a β-lactamase covalent labelling probe through reaction of a quinone methide moiety with nearby nucleophilic proteins and enzymes in 2016 (Scheme 9).[87] In the reported molecular probe, the core structure is based on cephalosporin ring coupled to a coumarin which functions as the fluorophore. Through cephalosporin amide bond cleavage and the coumarin fragment released, quinone methide, a highly reactive Michael acceptor was generated, and allowed covalent bonding with electron donors. This linkage of the probe with the donor moiety hence achieved proteins and enzymes localization as well as triggered fluorescence turn-on, as shown by their fluorescence emission spectrum and *in vitro* bacteria labelling.

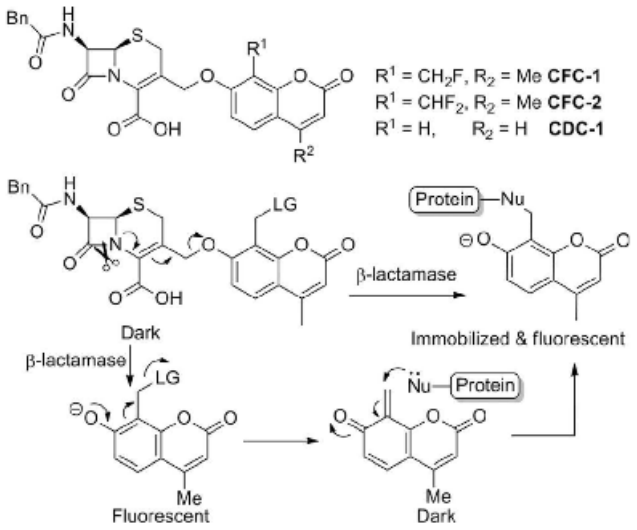

Scheme 9. Covalent labelling of nucleophilic proteins through cleavage of β–lactam ring, therefore generating fluorescence

Xing in 2017 published a paper on selective localization of class C β-lactamase (AmpC Bla) producing bacteria over class A (TEM-1 Bla) (Scheme 10).[65] Cephalosporin was covalently linked to a 4-aminothiophenol linker, followed by a tetraphenylethylene (TPE) fluorophore. Aggregation of the TPE moiety after AmpC interaction induced the desired off-on signal. To achieve selectivity towards only AmpC Bla and resistance to TEM-1 Bla, a bulky methoxyimino moiety at the 7'-position of β-lactam ring was utilized. Since TEM-1 Bla has a smaller binding pocket, inclusion of the bulky group in the probe design blocks TEM-1 Bla from interacting, resulting in the observed selectivity.

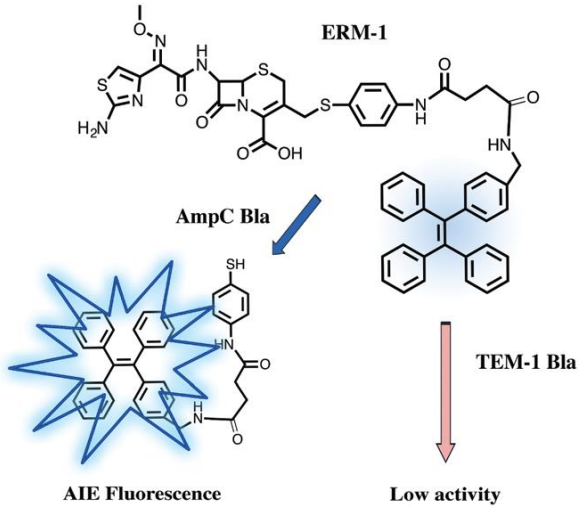

Scheme 10. Selectivity of AmpC over TEM-1 through incorporation of bulky group

Of the different types of β-lactamases, class A and C β-lactamases are more abundant and infect human community more often.[58, 88] However, class C β-lactamases are less studied comparing to its class A counterpart.[73, 89-90] This is a critical problem that needs to be addressed due to the rising number of cases regarding class C β-lactamases widespread resistance.[91-92] The resistance comes from the plasmid transfer of class C enzymes to bacteria strains such as *Escherichia coli* that were once class C β-lactamases negative. This leads to a greater degree of antibiotic therapeutic failure in clinical studies. Therefore, sensitive recognition of class C β-lactamase activity will be of paramount importance for identification of resistant bacteria, and to attain a well understanding of their molecular mechanism for improved therapeutic success.

1.5 Gaps and Proposed Work

Previously, experts from the industries had taken action with the development of novel drug derivatives as a direct outcome of antibiotics resistance. However, as drug creation is an extensive and tedious process that is both costly and does not guarantee success, many companies had been driven to cease invention of those short

term infection medications and move towards drugs for long term diseases to avoid unjustified profitability over total investment.[93] With no new antibiotics for resistance bacteria treatment, long term vision lies in the in-depth understanding of the resistance mechanism. This enables a better understanding of invasion mechanism and thus progress towards the mission of providing insights on alternative efficacious treatment methods.

Additionally, among the β-lactamase enzyme classes, class A and C Blas are considered the most significant in hydrolysis of β-lactam drugs by resistance bacteria transmitting in the human communities.[60, 74] Class A β-lactamases have been widely investigated.[55, 64, 94-96] Critically, recent outbreaks of resistance in bacterial species previously not expressing class C Blas, have emerged due to conjugative transmission of bacterial plasmid, which led to heightened clinical risk of antibiotic resistance in hospitals globally.[70, 72-73, 76] Although a similar serine hydroxyl group and geometries of active sites are observed in both class A and C Blas enzymes, their detailed secondary structures indicated a significance difference in the pocket size and the amino acid residue arrangement.[97-99] Therefore, a simple and unique approach that is capable of selectively identifying class C Blas enzyme activities will be clinically important in combatting microbial resistance.

In order to address the existing problem of limited class C investigations along with the challenge of rising number of class C resistance clinical cases, the second thesis chapter will present a project specific to selective labeling of bacterial species expressing class C β-lactamases, specifically to AmpC, for the effective early detection in clinical studies to address the resistant bacteria targeting gaps.

Chapter II. Unique Fluorescent Imaging Probe for Bacterial Surface Localization and Resistant Enzyme Imaging

2.1 Introduction

Widespread of antibiotic resistance among pathogenic bacteria is a critical problem currently faced by both hospital and community health worldwide, thus placing individuals' health at stake on both international and national scale.[93, 100-101] The significant reduction of antibiotics efficacy due to the production of β-lactamases (Blas) urge extensive investigations, as discussed in Chapter I.[102-106] Additionally, the development of specific approaches for selective recognition of resistance bacteria to gain a better understanding of the biochemical processes conferring bacterial drug resistance will be highly desirable.

Over the years, various effective strategies have been developed to facilitate Blas drug resistant enzyme investigations.[107-111] Among which, fluorescence optical imaging has been widely employed.[112-113] Despite the great dependability, most of the established methods through chemical-based probe molecules may have concerns for real-time monitoring of the dynamics of enzyme functions, or limited precision for accurate detection of bacterial resistant processes within a targeted and localized region which is mainly attributed to the multi-dimensional, heterogeneous and spatial complexity of the cellular environment. Moreover, the inevitable diffusion of chemical probe during the imaging process may present the potential issue of specificity or limited spatial resolution for real-time imaging analysis in living systems. Although several localization strategies based on covalent labelling or enzyme triggered probe molecule aggregation have been previously proposed to selectively report different resistant enzyme expression in bacterial pathogens,[65, 85, 114-

[115] these methods may potentially induce perturbation towards bacterial structure and functions in living settings. Therefore, the development of a simple and efficient method that allows effective probe localization on the bacterial surface, especially for the analysis of drug resistance bacteria, remains a technical challenge in the field and extensive studies are required.

Fatty acid lipid molecules are naturally expressed cell surface components that are well recognized as integral membrane structures with a close relation to cell wall stiffness and susceptibility to various types of cell functions.[116-117] So far, incorporation of fatty acid lipidated groups with therapeutic moieties and contrast agents have been proposed to achieve enhanced pharmacokinetic profile, improved treatment efficacy, as well as cellular structure-localized imaging to track real-time enzymatic dynamics and subcellular organelles position.[118-123]

2.2 Recent Studies on Lipid for Cell Membrane Targeting

Schultz and coworkers in 2009 developed a membrane targeting probe LaRee1 for monitoring of the pulmonary inflammation activities in cells (Scheme 1).[124] The reporter molecule which was based on the amino acid sequence PLGLEEA, cleaved selectively upon detection of a specific metalloproteinase, MMP12 implicated in inflammation. Conjugation of a palmitic acid to the N terminus, coumarin, and TAMRA yield the probe. Under the presence of MMP12, LaRee1 FRET pair breaks down producing fluorescence signals. The cleaved LaRee1 targeted to the plasma membrane, allowing detection of cell membrane light up. Further incubation allows fluorescence signals to be observed internally. In this study, palmitic acid allowed internalization to occur and enabled the detection of MMP12 activities which will be tedious with free-floating reporters.

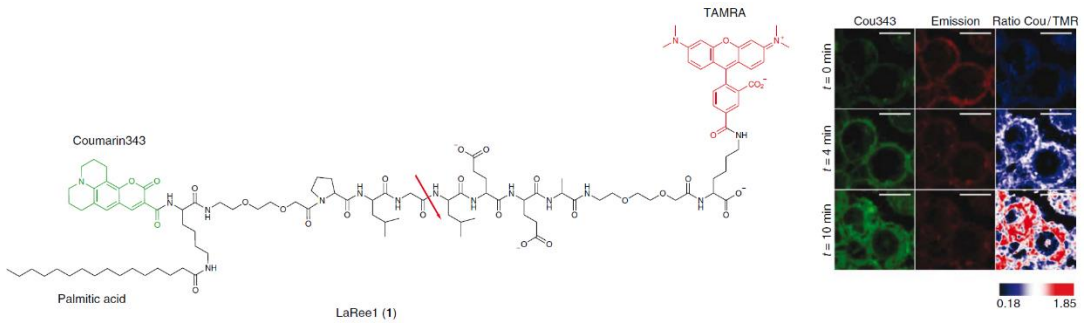

Scheme 1. Labelling of cell membrane for monitoring of pulmonary inflammation

In 2016, Ojida's group synthesized a fluorescence probe for the detection of histamine secreted during mast cell degranulation (Scheme 2).[125] The reporter molecule was synthesized through coupling of a Co(II) to a lipidated cyanine fluorophore. The presence of the Co(II) suppressed the fluorescence of cyanine. The introduction of lipid to the probe design allows the reporter to anchor itself onto the cell membrane surfaces for effective detection of histamine release. Upon the attachment of 3-Co(II) onto the cell membrane, the release of histamine during degranulation showed the coordination displacement of Co(II) which bound to the secreted histamine and enabled cyanine fluorophore switch on, generating real time responses.

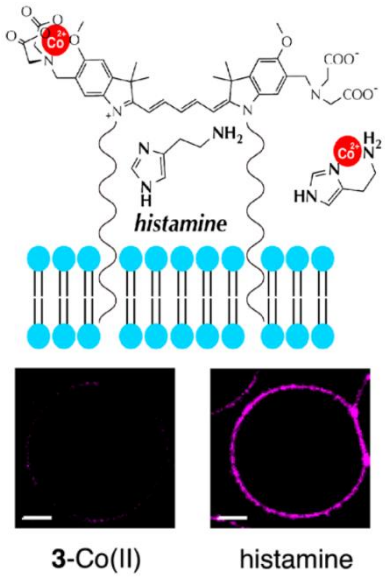

Scheme 2. Anchoring cell membrane for detection of secreted histamine

Haldar developed a novel vancomycin derivative that possess stronger and broader spectrum of antibacterial activities in 2014 (Scheme 3).[126] Through the simple addition of a cationic lipid moiety to vancomycin, the effectiveness increases significantly, at approximately 1000-folds. The study found a significant increase in susceptibility of bacteria to vancomycin with the incorporation of the lipid chain. The group studied the observation and found the effect to be a result of perturbation of the bacterial cell membrane by the cationic lipid which increases the efficiency of vancomycin in targeting vancomycin-resistant bacterial species. Compound 4-7 showed notable degree of permeabilization, while compound 1-3 had low to no changes. This shows the importance of chain length to anchor onto bacterial membrane for an improved antibacterial activities.

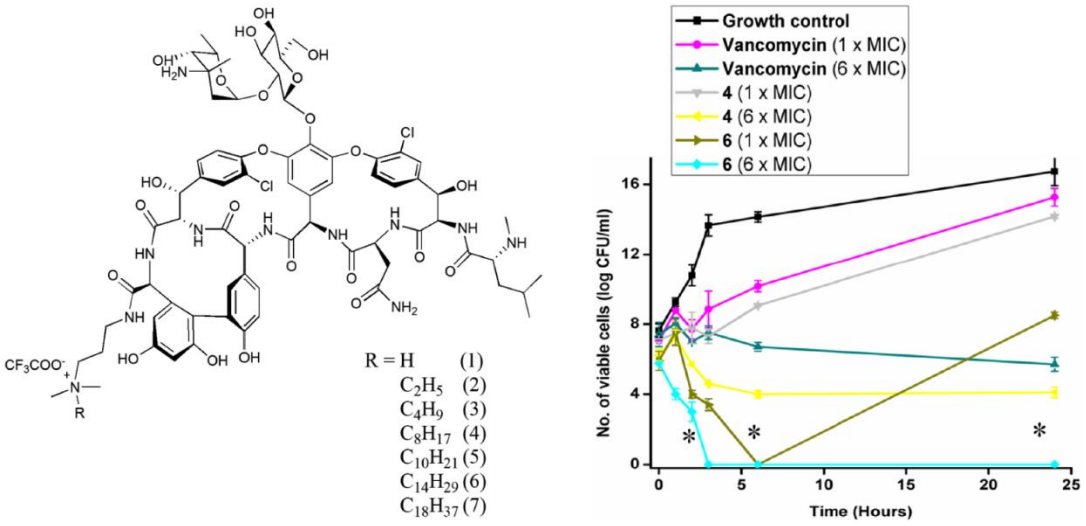

Scheme 3. Targeting surface membrane of vancomycin resistant bacteria

Mingeot-Leclercq in 2014 studied an aminoglycoside (neamine) conjugated with carbon chains for an improved drug activities towards multidrug resistant gram negative bacteria (Scheme 4).[127] A long and linear nonyl chain was utilized to bind LPS and induce bacterial outer membrane permeabilization. The incorporation of lipid into the design allowed bactericidal at its MIC with the ability to inhibit biofilm formation.

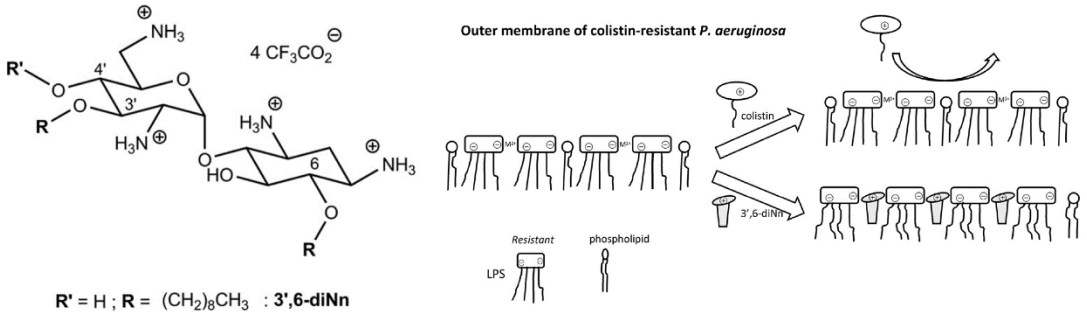

Scheme 4. Aminoglycoside derivative developed for improved antibacterial activities

2.3 Reporter Molecule Design

Inspired by the promising capability of such unique cell surface components, in this study, we present an effective method that can selectively recognize class C drug resistant Blas, and more importantly, interacts with bacterial cell components allowing the desired localization effect to be obtained (Scheme 5). Effective immobilization of the probe onto the bacterial surface was achieved through insertion of the lipidated fatty acid chain, which is a part of the cell membrane component favourable structure. Typically, a FRET pair, fluorescein isothiocyanate (FITC) fluorophore as donor and 4-(4,2-dimethylaminophenylazo) benzoic acid (DABCYL) as quencher, can be utilized to amplify enzyme activity. Under the presence of class C Blas (e.g. AmpC), the cephalosporin β-lactam ring in **DFD-1** was cleaved, releasing the 3'-position conjugated DABCYL. Such enzyme triggered probe release led to fluorescence enhancement and allowed real-time visualization of resistance bacteria. To attain AmpC enzyme selectivity, a bulky dibenzocyclooctyne (DBCO) group was attached to the cephalosporin β-lactam ring 7'-position to introduce steric hindrance, which may enable selective recognition towards AmpC Blas. More importantly, through fatty acid chain exploitation, insertion of the lipid into the bacterial surface can allow the observation of a desired localization. To achieve such localization property, we employed a lipid-azide conjugate for its penetration into the bacterial cell

surface, followed by copper-free click chemistry which immobilized the fluorescence signal onto the bacterial surface. Such a unique strategy can promote efficient localization of the fluorescence probe **DFD-1** and can thus greatly reduce the active diffusion of the probe molecules in bacterial structures, therefore providing great promise for performing precise and reliable screening of bacterial resistance in clinical practice.

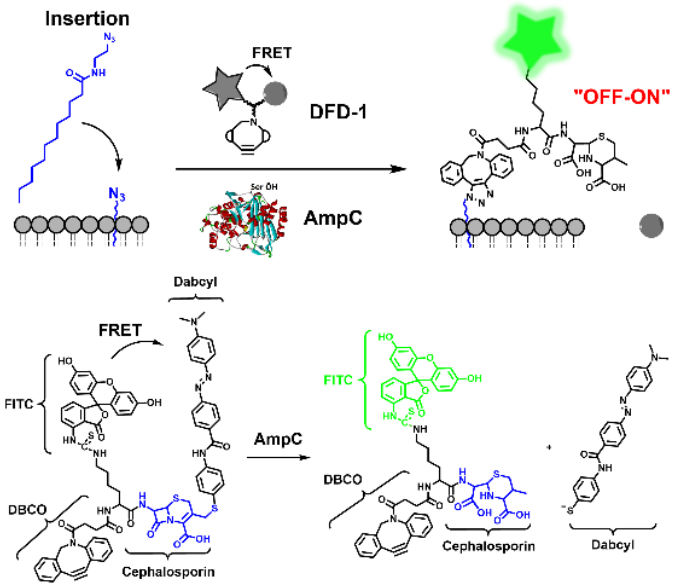

Scheme 5. Bacterial surface localization and enzymatic responsive fluorescence changes upon the reaction of probe **DFD-1** and AmpC Blas.

2.4 Results and Discussion

Synthetic Strategy. The synthetic route of probe **DFD-1** was depicted in Scheme 6. Cephalosporin β-lactam **1** was first linked with Mtt-Lys **3** at the 7'-position to yield Mtt-Lys-Lac **4** (step a). Next, at the 3'-position, cephalosporin was coupled with Thio-DABCYL **8** (prepared from trityl-protected 4-aminothiophenol with DABCYL) to afford **9** (step b). Subsequently, at the 7'-position of **9**, FITC was conjugated under basic reaction conditions, which was then followed by installation of the DBCO moiety through amide coupling with dibenzocyclooctyne-*N*-

hydroxysuccinimidyl ester (DBCO-NHS ester) to give the desired product **DFD-1**. The reaction mixture was purified by high performance liquid chromatography (HPLC) and characterized by mass spectroscopy analysis (MS).

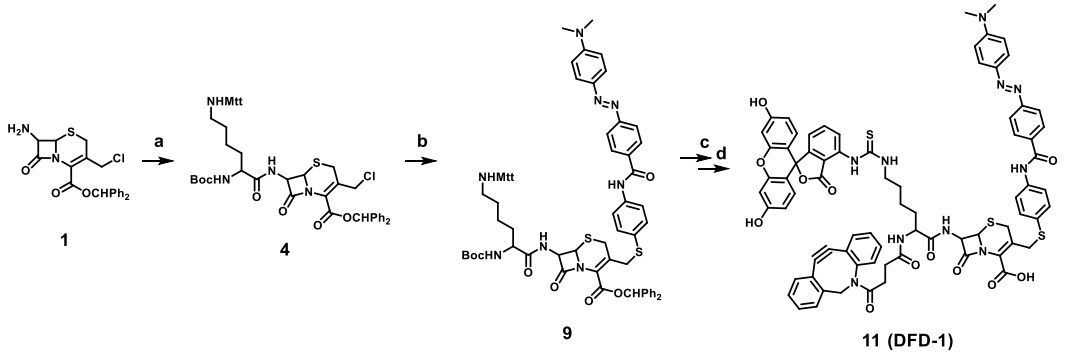

Scheme 6. Synthesis of the enzyme responsive probe **DFD-1**. Reagents and conditions: a) Mtt-Lys **3**, EDC.HCl, HOBt, TEA, CH_3CN:Dioxane (1:1), 0 °C - 23 °C, 12 h; b) Thio-DABCYL **8**, 2,6-Lutidine, NaI, DMF 23 °C, 13 h; c) i) 2 % v/v TFA, CH_2Cl_2, 23 °C, 1 h; ii) FITC, TEA, DMF, 23 °C, 10 h; d) i) 12.5 % v/v TFA, 2.5 % v/v TIPS, CH_2Cl_2, 23 °C, 4 h; ii) EDC.HCl, 4-DMAP, DBCO-NHS, DMF, 23 °C, 10 h.

Enzymatic Properties. To study the enzyme activity of the reporter molecule **DFD-1**, the fluorescence emission was recorded upon the addition of AmpC Blas in phosphate buffered saline (PBS) solution (0.1M, pH = 7.4). As shown in Figure 1A, under the absence of Blas enzyme, little fluorescence was observed with **DFD-1** alone due to the efficient FRET quenching. Notably, with the treatment of AmpC enzyme in PBS, significant enhancement in the fluorescence intensity at 516 nm was detected (~ 67-folds) before and after the enzyme reaction. This indicates the ability of AmpC Blas enzyme to efficiently cleave the β-lactam ring and release the quencher from the cephalosporin structure, thereby resulting in the observed intensity increment.

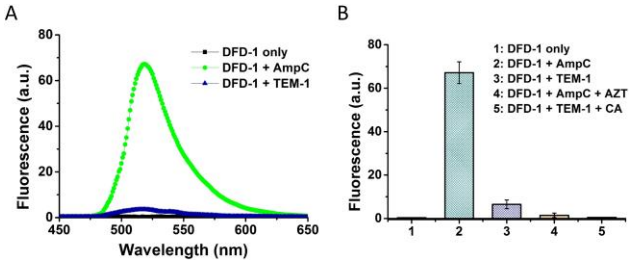

Figure 1. Emission spectra of A) probe **DFD-1** (10 μM) before and after incubation with AmpC and TEM-1 Blas, respectively (30 nM); B) Fluorescence enhancement of **DFD-1** incubated with AmpC, TEM-1 enzymes, inhibitor AZT and CA (100 μM) in 0.1M PBS (pH = 7.4).

Moreover, such enzyme cleavage is further supported by the LC-MS spectral analysis of the fragments corresponding to the hydrolysed cephalosporin ring and quencher Dabcyl moieties at 1062.73 and 377.23 respectively (Figure 2).

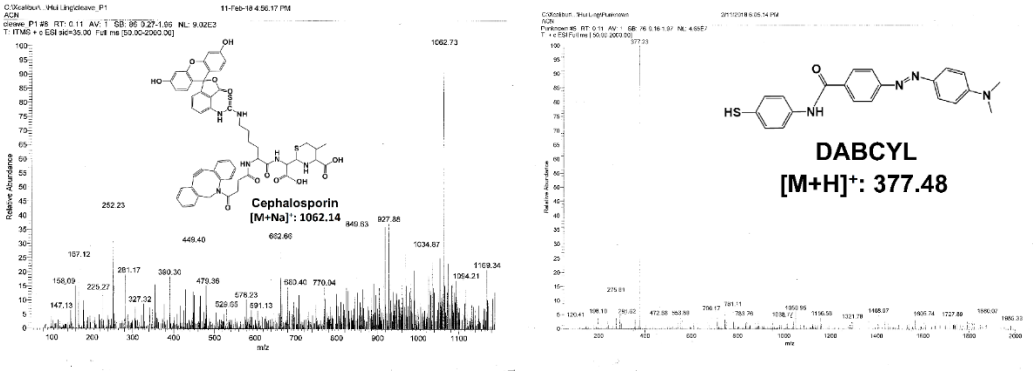

Figure 2. LC-MS of **DFD-1** cleavage with AmpC (500 nM).

In addition, a low fluorescence enhancement was found in the presence of a typical AmpC inhibitor, aztreonam (AZT) (Figure 1B). Such effective suppression of the AmpC enzymatic activity resulted in a substantial reduction in the fluorescence readout, which clearly demonstrates the specificity of **DFD-1** to AmpC enzyme instead of the spontaneous degradation of the probe or non-specific interactions. As a control, a similar enzymatic analysis was carried out with the use of TEM-1 enzyme, a typical class A Blas, to investigate the reaction selectivity. As shown in Figure 1A and 1B, treatment with TEM-1 enzyme showed a weak fluorescence activity after

enzyme reaction. Further analysis of enzyme kinetics was also conducted to determine the activity of both AmpC and TEM-1 Blas (Figure 3). The probe **DFD-1** cleavage was identified with the Michaelis constant, K_m = 7.4 μM and 10.0 μM, and the catalytic constant k_{cat} = 142.9 min^{-1} and 47.6 min^{-1} for AmpC and TEM-1 respectively. Hence, these results clearly demonstrated that the synthesized **DFD-1** exhibited a greater specificity and selectivity recognition towards AmpC Blas rather than to the TEM-1 counterpart, mostly attributed to the additional bulky DBCO moiety within **DFD-1** cephalosporin 7'-position that could accommodate well into the larger binding pocket located in AmpC Blas enzyme structure.[18-20]

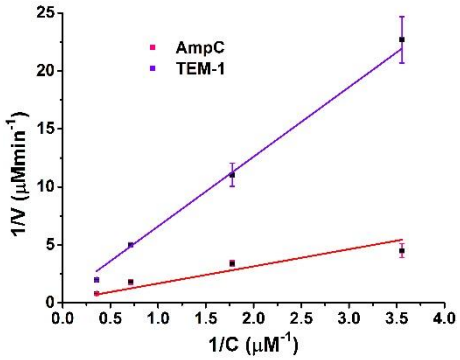

Figure 3. Enzyme kinetics of **DFD-1** to AmpC and TEM-1 Blas.

Ability of Lipids to Anchor onto Bacterial Surface. To investigate the feasibility of the enzyme responsive probe molecule to be efficiently anchored onto the bacterial surface for facilitated cell structure immobilization, we first employed a fatty acid molecule, an intrinsic lipid component of bacterial surface as the targeting moiety modified with an azide group, for incubation with the bacterial pathogens. As a proof of concept in this study, two commonly used bacterial strains, the gram negative *Pseudomonas aeruginosa* PAO1 (*P. aeruginosa* PAO1) and gram positive *Enterococcus faecium* (*E. faecium*) were chosen. Both are well-known as typical pathogens for bacterial resistance studies.[128-131] Upon bacterial incubation with the

lipid, a simple fluorescence molecule, DBCO-FITC (**DF**, Scheme 7), was subsequently conjugated through copper-free click reaction.

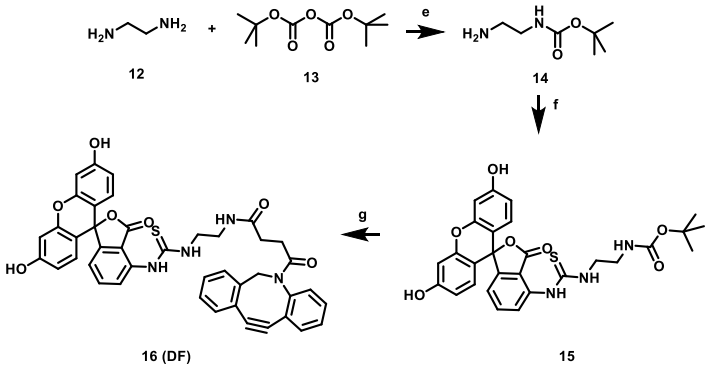

Scheme 7. Synthesis of desired **DF**. Reagents and conditions: e) CH_2Cl_2, 0 °C - 23 °C, 14 h; f) FITC, TEA, DMF, 23 °C, 10 h; g i) 30 % v/v TFA, CH_2Cl_2, 23 °C, 1 h; g ii) DBCO-NHS, DIPEA, DMF, 23 °C, 10 h.

Furthermore, to examine whether the lipid moiety chain length may affect bacterial insertion, the azido-coupled fatty acids with different carbons (N-(2-azidoethyl) stearamide, N-(2-azidoethyl) dodecanamide, and N-(2-azidoethyl) hexanamide abbreviated as **LA-18**, **LA-12**, and **LA-6** respectively; Scheme 8) were also synthesized and their subsequent bacterial incubation were carried out for imaging analysis.

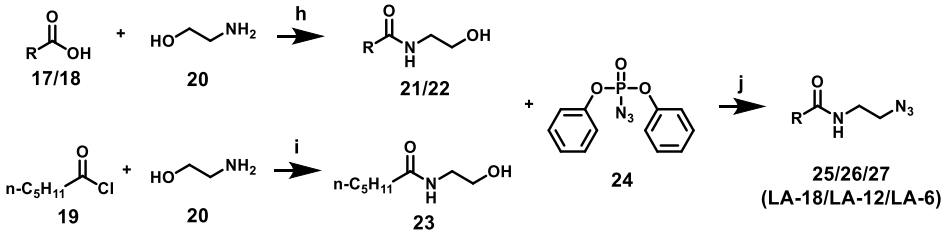

Scheme 8. Synthesis of lipid-N_3 **LA-18/LA-12/LA-6**. Reagents and conditions: h) Ethyl chloroformate, TEA, CH_2Cl_2, 0 °C–23 °C, 2 h; i) TEA, CH_2Cl_2, 23 °C, 1 h; j) DBU, DMF, N_2, 120 °C, 2 h.

The fluorescence images were recorded to investigate the effective bacterial surface insertion by using confocal microscopy with the excitation at 488 nm (Figure 4A).

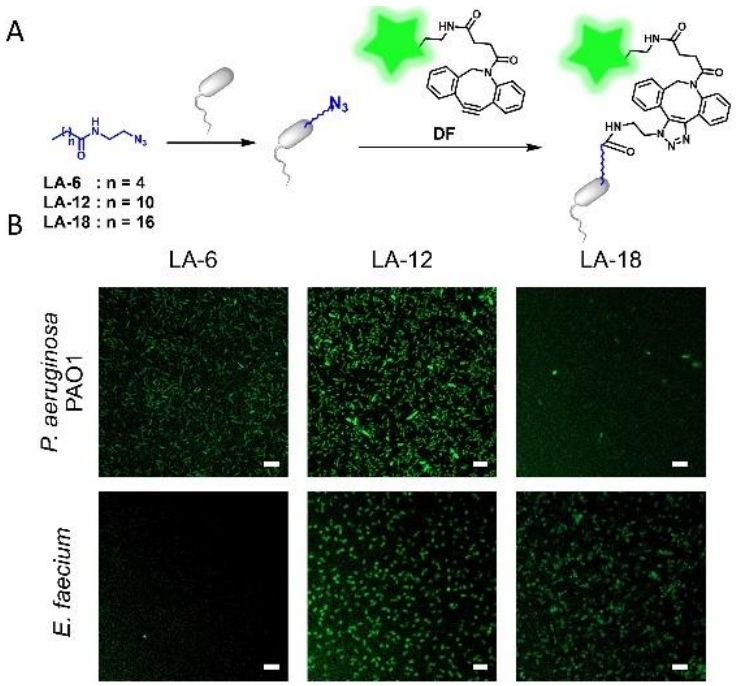

Figure 4. A) Scheme of bacterial insertion with lipid of **LA-18, LA-12** and **LA-6**, followed by click reaction with **DF**; B) Confocal imaging of lipid screening in *P. aeruginosa* PAO1 and *E. faecium* bacterial strains upon treatment of lipid moieties (**LA-18, LA-12** and **LA-6**) (2 μM) and **DF** (2 μM) in 0.1 M PBS, pH = 7.4. Scale bar: 5 μm.

As shown in Figure 4B, *P. aeruginosa* PAO1 strain, there was a weak fluorescence observed in fatty acid moiety **LA-18** incubated bacteria when compared to the pathogens treated with **LA-6** and **LA-12** structures. Although both bacteria treated with **LA-6** and **LA-12** moieties led to an increment in fluorescence signal, **LA-12** exhibited a stronger fluorescence intensity than that of **LA-6**. Similarly, for the *E. faecium* bacteria, among three fatty acids moieties, **LA-12** demonstrated the strongest fluorescence for lipid facilitated bacterial imaging (Figure 4B and Figure 5).

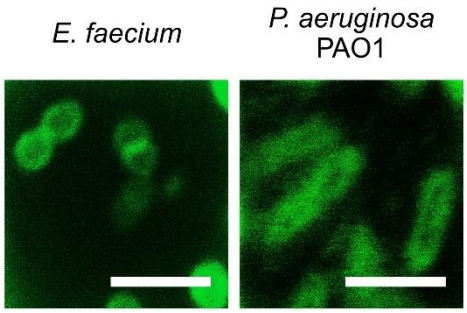

Figure 5. Fluorescence imaging of *E. faecium* and *P. aeruginosa* PAO1 outer membrane insertion through incorporation of **LA-12** (2 μM) and subsequent incubation of **DF** (2 μM) in 0.1 M PBS, pH = 7.4. Scale bar: 5 μm.

The results indicated that the increased length of the carbon chain could likely enhance the immobilization of the probe onto the bacterial surface. The shorter hydrophobic chain in **LA-6** would lead to less staining, which could be easily washed away, giving the decreased fluorescence intensity. Although **LA-18** could also show an enhanced tracking ability on the bacterial surface, this azido-coupled lipid moiety indicated limited solubility in aqueous solutions, which may potentially affect cell activity and reduce the effective concentration for bacterial imaging. These fluorescent staining studies in both *P. aeruginosa* PAO1 and *E. faecium* bacteria clearly showed the lipid moiety **LA-12** as the ideal tracer to specifically immobilize **DF** onto the bacterial cell surfaces, which may thus greatly facilitate dynamic visualization of drug-resistant enzymes in living bacteria. Additionally, staining of **LA-12** treated bacterial strains with propidium iodide (PI) showed minimum bacterial perturbation (Figure 6). These studies unequivocally indicated the great possibilities of **LA-12** as a promising localizing agent for bacterial imaging in living conditions.

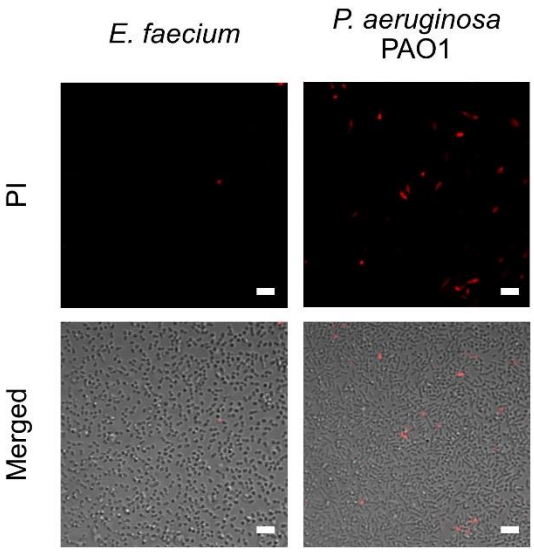

Figure 6. Confocal imaging utilizing PI as a bacterium cell viability indicator. Bacterial strains were firstly incubated for 1 h with **LA-12** (50 μM), washed and followed by a 0.25 h incubation with PI (10 μM) in 0.1 M PBS, pH = 7.4. Scale bar: 5 μm.

Moreover, the MIC experiment conducted on LA-12 shows minimum toxicity towards the bacteria tested (Table 1). This showed the possibility of utilizing LA-12 as a benign and simple method for cell membrane surfaces targeting, to monitor and detect enzyme and environmental changes.

Bacterial strain type	**MIC of LA-12 (μg mL^{-1})**
S. aureus	> 128
MRSA BAA-44	> 128
P. aeruginosa PAO1	> 128

Table 1. MIC is defined as the lowest concentration needed to induce bacterial growth inhibition. The bacterial strains were incubated in BHI broth with different concentration of **LA-12** for 18 h. The MIC values were determined from OD_{600}, with the OD_{600} value of the culture with absence of bacteria used as the control.

Imaging Resistant Bacterial with LA-12 and DFD-1. Encouraged by the specific enzymatic hydrolysis of **DFD-1** as well as the promising bacterial immobilization ability of **LA-12** lipid moiety, we investigated the possibility for the localization of the reporter molecular **DFD-1** onto the bacterial surface for real-time imaging of drug resistant enzyme in living bacterial pathogens (Figure 7). In this typical study, two antibiotic resistant bacterial strains *Enterobacter cloacae* (*E. cloacae*, ATCC 13047) and *P. aeruginosa* PAO1 (ATCC 15692), were selected as our main targets primarily due to their native capability to produce class C AmpC Blas enzyme. Another two drug resistant bacterial pathogens *E. faecium* (ATCC 51559) and methicillin-resistant *Staphylococcus aureus* (MRSA BAA-44, ATCC BAA44) were utilized as control strains owing to their high expression levels of class A TEM-1 Blas. In addition, two antibiotic susceptible strains *Pseudomonas putida* OUS82 (*P. putida* OUS82) and *Staphylococcus aureus* (*S. aureus*, ATCC 29213) without Blas expression were selected as the negative control. Typically, these bacterial strains were separately treated with lipid **LA-12** for 1 h at 37 °C. After washing and subsequent incubation with **DFD-1** probe for another 30 min, the bacterial samples were subjected to confocal microscopy for fluorescence imaging analysis. As shown in Figure 7, strong fluorescence emissions were observed upon the incubation of **DFD-1** probe with AmpC Blas enzyme producing bacterial strains in *P. aeruginosa* PAO1 and *E. cloacae*. On the other hand, similar bacterial treatment with **LA-12** and **DFD-1** in TEM-1 Blas enzyme expressing MRSA BAA-44 and *E. faecium* strains only resulted in weak fluorescence signals.

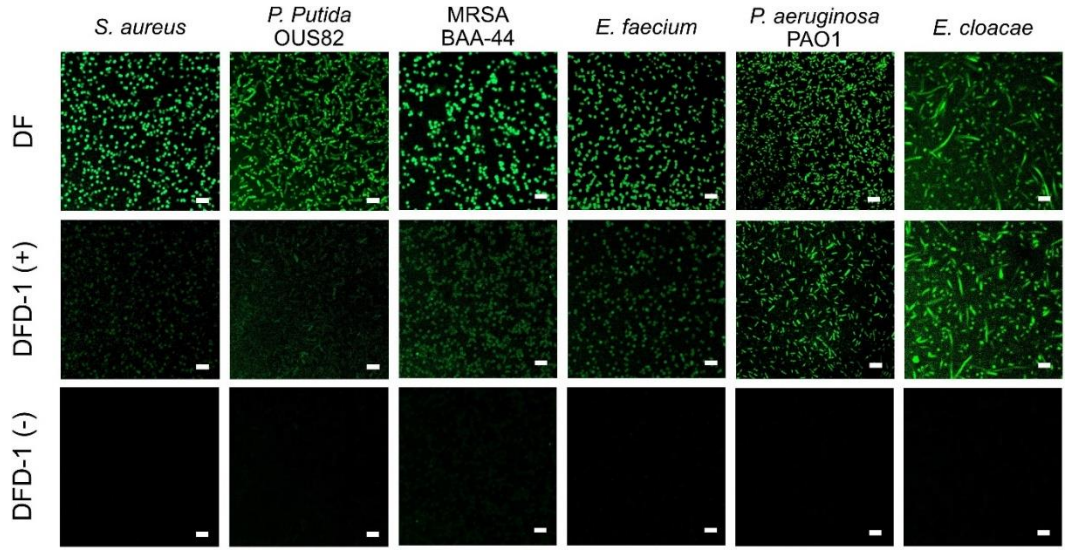

Figure 7. Fluorescence imaging of selective enzyme reaction and bacterial surface localization in living bacteria: antibiotic susceptible strains *S. aureus* and *P. putida* OUS82, TEM-1 Blas producing MRSA BAA-44 and *E. faecium*, as well as AmpC Blas producing *P. aeruginosa* PAO1 and *E. cloacae*, with subsequent treatment of **LA-12** (50 μM) and **DFD-1** (10 μM) in 0.1 M PBS, pH = 7.4. Scale bar: 5 μm.

Importantly, the pre-treatment of targeted strains producing AmpC enzyme (e.g. *P. aeruginosa* PAO1) with typical class C Blas AZT inhibitor greatly reduced the fluorescence intensity in bacterial imaging, while similar incubation of *P. aeruginosa* PAO1 bacteria with class A TEM-1 enzyme inhibitor CA demonstrated little effect on the fluorescence signal (Figure 8).

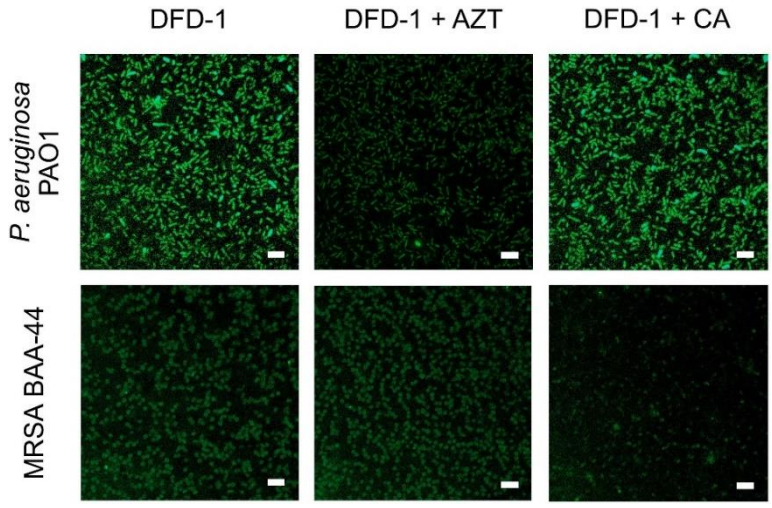

Figure 8. Confocal imaging of MRSA BAA-44 and *P. aeruginosa* PAO1 enzymatic inhibition with CA or AZT inhibitor (100 μM) and **LA-12** (50 μM), followed by **DFD-1** (10 μM) in 0.1 M PBS, pH = 7.4. Scale bar: 5 μm.

In the negative control, there was almost no fluorescence detected in antibiotic susceptible *S. aureus* and *P. putida* OUS82 bacteria under the treatment with the probe molecule (Figure 7). Importantly, there was minimum effect observed in inhibition of bacterial growth during the bacterial imaging by using **DFD-1** probe molecule (Table 2). These results clearly enforced the capability of the designed enzymatic substrate **DFD-1** as a safe probe molecule for the selective recognition of AmpC enzyme activities in live bacterial strains.

Bacterial strain type	**MIC of DFD-1 (μg mL^{-1})**
S. aureus	> 128
MRSA BAA-44	> 128
P. aeruginosa PAO1	> 128

Table 2. The bacterial strains were incubated in BHI broth with different concentration of **DFD-1** for 18 h. The MIC values were determined from OD_{600}, with the OD_{600} value of the culture with absence of bacteria used as the control.

Moreover, compared to the imaging of bacteria strains treated with **LA-12** lipid moiety and **DF**, the bright fluorescence signals observed in *P. aeruginosa* PAO1 and *E. cloacae* strains further confirmed the localization ability of **LA-12** that facilitated immobilization of the enzyme responsive probe onto the bacterial surface. (Figure 7 and Figure 9).

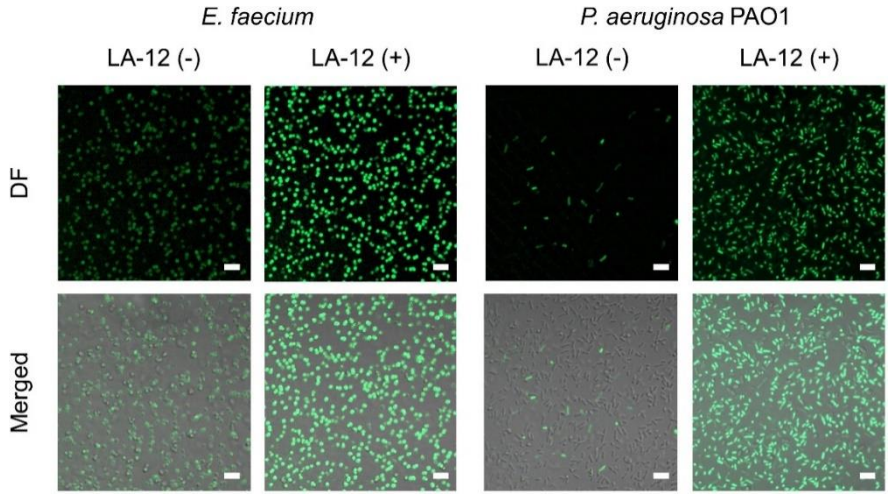

Figure 9. Fluorescence imaging of *E. faecium* and *P. aeruginosa* PAO1 with or without **LA-12** (50 μM) incubation, followed by **DF** (10 μM) in 0.1 M PBS, pH = 7.4. Scale bar: 5 μm.

Enzyme Activity and Click Reaction Contribution towards Imaging. In order to investigate the fluorescent staining effects of enzyme hydrolysis and click chemistry triggered bacterial localization contributed to live bacterial imaging, we compared these individual performances in the drug resistance bacteria (e.g. *P. aeruginosa* PAO1) with AmpC Blas expression. In this typical study, the bacterial strain *P. aeruginosa* PAO1 was first incubated with **LA-12** lipid moiety for 1 h at 37 °C, followed by subsequent addition of **DF** (Figure 10A). The bacterial surface immobilization triggered by copper free click chemistry reaction was determined by measuring the fluorescence change at different time durations. Alternatively, the enzyme cleavage activity was also carried out in a similar manner, through incubation of **LA-12** lipid-labelled *P. aeruginosa* PAO1 bacteria with the probe **DFD-1**, the fluorescence change was recorded to evaluate surface localized enzyme activities. As shown in Figure 10B, under the same reaction conditions, **DF** labelling triggered by click reaction exhibited a relatively higher fluorescence intensity than the fluorescence generated from the enzyme reaction. The fluorescence profiles implied

that both enzyme hydrolysis and click chemistry triggered surface insertion would contribute to the bacterial imaging, and the click coupling would facilitate the imaging probe staining on bacterial surface for effective imaging studies. (Figure 10).

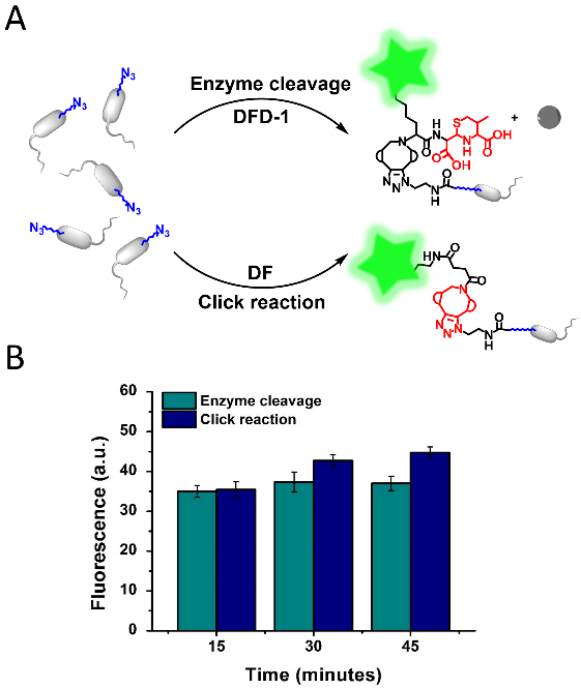

Figure 10. A) Scheme of the different staining effects from the enzyme hydrolysis and click reaction towards fluorescence imaging in live bacteria; B) Comparison of fluorescence intensity between the enzyme hydrolysis and click chemistry in live bacteria. **LA-12** lipidated (50 μM) *P. aeruginosa* PAO1 strains were separately treated with **DF** and **DFD-1** (10 μM), under different time interval in 0.1 M PBS, pH = 7.4.

Flow Cytometry Analysis. Additionally, we studied the possibility to quantify the specific labelling of AmpC Blas expressing resistant bacteria (e.g. *P. aeruginosa* PAO1) using flow cytometer analysis (FCM). The antibiotic susceptible *S. aureus* and resistant MRSA BAA-44 strains with expression of TEM-1 Blas were used as the negative control (Figure 11). In this study, the different strains were first incubated with **LA-12** moiety and subsequently treated with **DFD-1** for flow cytometry analysis.

Fluorescence signals were collected at 525 nm. As shown in Figure 11A, a stronger intensity of fluorescence was observed in AmpC expressing *P. aeruginosa* PAO1 strain compared to the negative control *S. aureus* bacteria that do not produce β-lactamase. Meanwhile, a lower fluorescence change was detected for TEM-1 producing MRSA BAA-44 strain. Moreover, a similar flow cytometry analysis with the treatment of AmpC enzyme inhibitor AZT, showed a significant decrease in the fluorescence intensity (Figure 11B). Therefore, these data clearly demonstrates the specificity of **DFD-1** as a reliable reporter molecule for quantification of AmpC activities in antibiotic resistance bacteria.

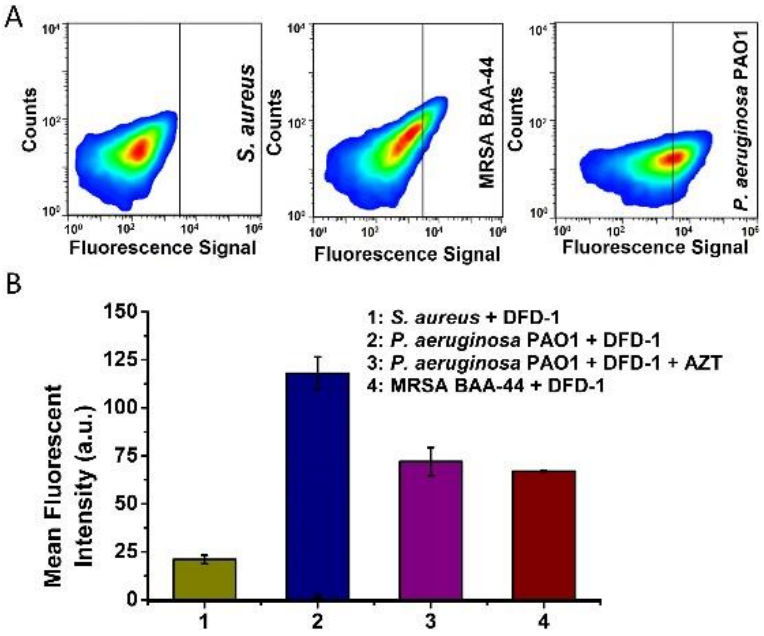

Figure 11. Flow cytometry analysis of resistant bacterial strains incubated with A) lipid **LA-12** (50 μM) and probe **DFD-1** (10 μM); B) lipid **LA-12** (50 μM) and inhibitor AZT (100 μM), followed by probe **DFD-1** (10 μM) staining in 0.1M PBS, pH = 7.4. Concentration of bacterial was approximately 10^8 cells mL^{-1}.

2.5 Conclusion

In conclusion, this work presented a specific and selective approach towards efficient bacterial surface localization and real-time imaging of drug resistant bacteria with AmpC enzyme expression. In this study, the optimized lipid moiety (**LA-12**) could efficiently be inserted into the bacterial surface and thus greatly facilitated the localization of the enzyme triggered fluorescent signal onto the bacterial surface. By taking advantage of the bulky DBCO group at the 7'-position of cephalosporin structure, the fluorescent probe **DFD-1** could selectively recognize AmpC Blas enzyme. The significant fluorescence enhancement towards selective detection of AmpC Blas enzyme indicated a promising strategy for direct observation of resistant bacterial infections in living conditions. More importantly, such lipid facilitated surface localization of fluorescence labelling could also provide the promising capability for dynamic monitoring of bacterial development and assessing effective anti-bacterial therapeutics *in vitro* and *in vivo*.

Chapter III. Experimental Section

3.1 General Informations

Cephalosporin β-lactam derivative **1** was purchased from Ostuka Chemical Co. Ltd.[85, 102] The purified AmpC β-lactamase was acquired from MyBioSource.[132] Purified TEM-1 β-lactamase was obtained from Biologics Process Development.[65] Other reagents were purchased from Sigma Aldrich. Commercially available reagents were used without further purification. Four bacterial strains *Enterobacter cloacae* (ATCC 13047), *Enterococcus faecium* (ATCC 51559), methicillin-resistant *Staphylococcus aureus* MRSA BAA-44 (ATCC BAA44), and *Staphylococcus aureus* (ATCC 29213) were purchased from American Type Culture Collection (ATCC). Two bacterial strains *Pseudomonas aeruginosa* PAO1 (ATCC 15692) and *Pseudomonas putida* OUS82 were gifted from Prof Yang Liang, School of Biological Sciences, Nanyang Technological University. ^{1}H NMR spectra were recorded using a Bruker Avance 400 spectrometer. Mass spectra (MS) were measured with Thermo LCQ Deca XP Max or Thermo Finnigan MAT 95 XP mass spectrometer for electrospray ionization mass spectra (ESI). Flash column chromatography was performed using Merck silica gel 60 with distilled solvents. Reverse-phase HPLC analysis was performed on a Shimadzu HPLC system using an Alltima C-18 (250 × 10 mm) column at a flow rate of 3.0 mL min^{-1} for preparation and a C-18 (250 × 4.6 mm) at a flow rate of 1.0 mL min^{-1} for analysis. Fluorescence emission spectra were performed on a Varian Cary eclipse Fluorescence Spectrophotometer. UV absorption spectra were recorded in a 10 mm path quartz cell on a Beckman coulter DU800 spectrometer. Fluorescence microscopic imaging and confocal laser scanning microscopic imaging were conducted with Zeiss LSM 800 Confocal Microscope.

3.2 General Procedures

General procedure for the synthesis of Mtt-Lys, 3

To a solution of 4-methyltriphenylmethyl chloride (4.00 mmol, 1.17 g) in dichloromethane/dimethylformamide (2:1, 3.0 mL) was added Boc-Lys-OH **2** (2.00 mmol, 493 mg) and triethylamine (8.0 mmol, 1.1 mL). The mixture was stirred vigorously for 4 hours. The reaction was quenched with 2.5 mL of methanol, extracted with ethyl acetate, water, and brine. The organic layer was subsequently dried over sodium sulfate, filtrated and evaporated to dryness. The crude was purified using silica gel column (ethyl acetate:*n*-hexane) to afford **3** as a white solid (593 mg, 59% yield). ^{1}H NMR (400 MHz, $CDCl_3$) δ (ppm): 1.19-1.27 (2H, m), 1.39 (9H, s), 1.43-1.53 (3H, m), 1.59-1.1.67 (1H, m), 2.30 (3H, s), 2.31-2.37 (2H, m), 4.02-4.06 (1H, m), 5.22-5.24 (1H, m), 7.09-7.43 (14H, m).

General procedure for the synthesis of Mtt-Lys-Lac, 4

To β-lactam derivative **1** (0.670 mmol, 278 mg) in acetonitrile/dioxane (1:1, 21.0 mL) was added 98.0 μL of triethylamine dropwise at 0 °C to obtain a clear solution. Mtt–Lys **3** (0.670 mmol, 337.0 mg), 1-hydroxybenzotriazole (1.34 mmol, 181 mg), and *N*-(3-dimethylaminopropyl)-*N'*-ethylcarbodiimide hydrochloride (1.68 mmol, 322 mg) were added sequentially. The reaction was carried out for 12 hours while warming up to 23 °C. The resultant mixture was evaporated and purified with silica gel column (ethyl acetate:*n*-hexane) to afford **4** as a yellow solid (223 mg, 37% yield). ^{1}H NMR (400MHz, $CDCl_3$) δ (ppm): 1.37 (2H, m), 1.40 (9H, s), 1.45-1.49 (2H, m), 1.54-1.58 (2H, m), 1.71-1.79 (1H, m), 2.10 (2H, t, J = 6.7 Hz), 2.28 (3H, s), 3.44

(2H, dd, J_1 = 18.3 Hz, J_2 = 49.0 Hz), 4.32 (2H, s), 4.95 (1H, d, J = 5.0 Hz), 5.03 (1H, d, J = 8.0 Hz), 5.79 (1H, dd, J_1 = 5.0 Hz, J_2 = 8.8 Hz), 6.96-7.46 (24H, m).

General procedure for the synthesis of Trt-Thio, 6

To a cooled to 0 °C trityl chloride (2.00 mmol, 558 mg) in 1.0 mL of dichloromethane was added 4-aminothiophenol **5** (2.20 mmol, 288 mg), followed by 0.40 mL of trifluoroacetic acid dropwise and stirred for 10 hours while warming up to 23 °C. The reaction was quenched with 3.0 mL of 1 M sodium hydroxide, extracted with ethyl acetate and three times brine. The organic layer was dried over sodium sulfate, filtered and evaporated to dryness. The crude was purified using silica gel column (ethyl acetate:*n*-hexane) to afford **6** as a white solid (735 mg, 100% yield). ^{1}H NMR (400MHz, $CDCl_3$) δ (ppm): 3.31 (2H, s), 6.30 (2H, d, J = 8.6 Hz), 6.74 (2H, d, J = 8.6 Hz), 7.14-7.40 (15H, m).

General procedure for the synthesis of Trt-Thio-DABCYL, 7

To DABCYL (0.250 mmol, 67.4 mg) in dichloromethane/pyridine (1:1, 5.0 mL) was added *N*-(3-dimethylaminopropyl)-*N'*-ethylcarbodiimide hydrochloride (1.00 mmol, 192 mg) and stirred for 10 minutes. Trt–Thio **6** (0.250 mmol, 91.8 mg) followed by 4-dimethylaminopyridine (0.0175 mmol, 2.2 mg) were subsequently added and stirred for 3 hours. The reaction mixture was concentrated and extracted with ethyl acetate, sodium bicarbonate, brine, and dried over sodium sulfate. The filtrate was collected and evaporated to dryness. The crude was purified using silica gel column (ethyl acetate:*n*-hexane) to afford **7** as an orange solid (71.2 mg, 46%). ^{1}H NMR (400MHz; $CDCl_3$) δ (ppm): 3.11 (6H, s), 6.76 (2H, d, J = 9.2 Hz), 6.97 (2H, d, J = 8.6 Hz), 7.19-7.91 (23H, m).

General procedure for synthesis of Thio-DABCYL, 8; Mtt-Lys-Lac-Thio-DABCYL, 9

To Trt-Thio-DABCYL **7** (0.100 mmol, 61.9 mg) in 2.5 mL of dichloromethane was added 25 μL of triisopropylsilane (1 % v/v) dropwise, followed by 750 μL of trifluoroacetic acid (30 % v/v) dropwise. The reaction was left to stir for 1 hour before concentration and washed three times with dichloromethane. The purple solid was subsequently dried over reduced pressure for 3 hours to obtain Thio-DABCYL **8** as a crude material.

To compound **8** in 2.5 mL of dimethylformamide was added 2,6-lutidine (0.200 mmol, 23.3 μL), Mtt-Lys-lactam **4** (0.100 mmol, 90.0 mg), and NaI (0.200 mmol, 30.0 mg). The reaction was stirred for 13 hours. The mixture was extracted with ethyl acetate, water, brine and dried over sodium sulfate, filtered and evaporated to dryness. The crude was purified using silica gel column (ethyl acetate:*n*-hexane) to afford **9** as an orange solid (78.1 mg, 63% yield). MS (ESI) m/z: 1239.12, calculated for $[M]^+$: 1239.56.

General procedure for the synthesis of FITC-Lys-Lac-Thio-DABCYL, 10

To Mtt-Lys-Lac-Thio-DABCYL **9** (0.040 mmol, 50.0 mg) in 1.0 mL of dichloromethane was added 20 μL of trifluoroacetic acid (2 % v/v) dropwise and stirred for 1 hour. The mixture was evaporated to dryness, washed three times with dichloromethane, and left to dry over reduced pressure for 3 hours.

To the crude in 500 μL of dimethylformamide was added FITC (0.060 mmol, 23.4 mg) and triethylamine (0.060 mmol, 8.4 μL). The reaction was left to stir for 10 hours. The reaction was extracted with ethyl acetate, water, brine, and dried over

sodium sulfate, filtered and evaporated to dryness. The crude was purified using silica gel column (methanol:ethyl acetate) to afford **10** as a red solid (5.5 mg, 10% yield). MS (ESI) m/z: 1373.04, calculated for $[M]^+$: 1372.60.

General procedure for the synthesis of DFD-1, 11

To a cooled to 0 °C of FITC-Lys-Lac-Thio-DABCYL **10** (0.0045 mmol, 6.2 mg) in 400 μL of dichloromethane was added 50 μL of trifluoroacetic acid (12.5 % v/v) and 10 μL of triisopropylsilane (2.5 % v/v). The reaction mixture was stirred for 4 hours. The mixture was evaporated to dryness, washed three times with dichloromethane, and left to dry over reduced pressure for 3 hours.

To the crude in 300 μL of dimethylformamide was added DBCO-NHS ester (0.011 mmol, 4.4 mg), and 2.4 μL of *N*,*N*-diisopropylethylamine. The reaction was left to stir over 10 hours and purified using reverse phase HPLC to afford **11** as a red solid (0.6 mg, 10% yield). MS (ESI) m/z: 1393.08, calculated for $[M]^+$: 1393.58.

General procedure for the synthesis of Boc-Amine, 14

To a stirred and cooled to 0 °C of ethylenediamine **12** (20.0 mmol, 1.34 mL) in 15 mL of dichloromethane was added a solution of di-*tert*-butyl dicarbonate **13** (2.00 mmol, 0.46 mL) in 10 mL of dichloromethane dropwise over 2 hours. The mixture was warmed up to 23 °C and stirred over 14 hours. The reaction was concentrated and dissolved in saturated sodium bicarbonate. The crude was extracted with dichloromethane three times, brine, and dried over sodium sulfate, filtered and evaporated to dryness to afford **14** as a yellow oil (320 mg, 100% yield). ^{1}H NMR (400MHz; $CDCl_3$) δ (ppm): 1.45 (9H, s), 2.80 (2H, t, J = 5.8 Hz), 3.16-3.22 (2H, m), 4.94 (1H, brs).

General procedure for the synthesis of Boc-Amine-FITC, 15

To Boc-Amine **14** (0.0706 mmol, 11.3 mg) in 500 μL of dimethylformamide cooled to 0 °C, was added FITC (0.0642 mmol, 25.0 mg) and 13.4 μL of trimethylamine. The reaction was stirred for 10 hours. The reaction was extracted with ethyl acetate, water, brine, and dried over sodium sulfate, filtered and evaporated to dryness. The crude was purified using silica gel column (methanol:ethyl acetate:*n*-hexane) to afford **15** as a yellow solid (24.7 mg, 70% yield). MS (ESI) m/z: 550.31, calculated for $[M]^+$: 549.60.

General procedure for the synthesis of DF, 16

To Boc-Amine-FITC **15** (0.0112 mmol, 6.2 mg) in 125 μL of dichloromethane was added 37.5 μL of trifluoroacetic acid (30% v/v) and stirred for 1 hour. The mixture was evaporated to dryness, washed three times with dichloromethane and left to dry over reduced pressure over 3 hours to give the crude material. The crude material in 62.5 μL of dimethylformamide was added DBCO-NHS ester (0.0226 mmol, 9.1 mg) and 5.9 μL of *N*,*N*-diisopropylethylamine. The reaction was left to stir for 10 hours and purified using reverse phase HPLC to afford **16** as a yellow solid (2.0 mg, 24% yield). MS (ESI) m/z: 737.33, calculated for $[M]^+$: 736.80.

General procedure for the synthesis of Amide-Alcohol, 21/22

To carboxylic acid **17** (5.00 mmol, 1.28 g) in 5.0 mL of dichloromethane was added 1.4 mL of triethylamine. The reaction mixture was subsequently cooled to 0 °C before the addition of 0.96 mL of ethyl chloroformate dropwise. The reaction was left to warm up to 23 °C and stirred for 2 hours. Subsequently, ethanolamine **20** (7.50 mmol, 0.46 mL) was added dropwise at 0 °C and stirred at 23 °C over 9 hours. The

mixture was evaporated to dryness. 10 mL of water was added and stirred for another 10 minutes before filtration and the filtrate was evaporated to dryness under reduced pressure. The crude was purified using silica gel column (methanol:ethyl acetate) to afford**:**

21 as a white solid (606 mg, 37% yield). ^{1}H NMR (400MHz; $CDCl_3$) δ (ppm): 0.88 (3H, t, *J* = 7.1 Hz), 1.25-1.29 (28H, m), 1.60-1.67 (2H, m), 2.21 (2H, t, *J* = 7.8 Hz), 3.41-3.45 (2H, q, *J* = 5.4 Hz), 3.73 (2H, t, , *J* = 4.8 Hz), 5.92 (1H, brs).

22 as a white solid (572.0 mg, 47% yield). ^{1}H NMR (400MHz; $CDCl_3$) δ (ppm): 0.88 (3H, t, *J* = 6.7 Hz), 1.26-1.29 (16H, m), 1.60-1.67 (2H, m), 2.20 (2H, t, *J* = 7.4 Hz), 3.41-3.45 (2H, m), 3.73 (2H, t, , *J* = 4.0 Hz), 5.92 (1H, brs).

General procedure for the synthesis of Amide-Alcohol, 23

To acyl chloride **19** (5.0 mmol, 0.70 mL) in 15 mL of dichloromethane was added dropwise of ethanolamine **20** (7.50 mmol, 0.46 mL). 1.40 mL triethylamine dissolved in 15 mL of dichloromethane was subsequently added. The reaction mixture was stirred for 1 hour before evaporated to dryness. The crude was purified using silica gel column (methanol:ethyl acetate) to afford **23** as a white solid (589 mg, 74% yield). ^{1}H NMR (400MHz; $CDCl_3$) δ (ppm): 0.82 (3H, t, *J* = 6.1 Hz), 1.19-1.24 (4H, m), 1.51-1.58 (2H, m), 2.13 (2H, t, *J* = 7.6 Hz), 3.29-3.32 (2H, m), 3.60 (2H, m), 4.31 (1H, brs), 6.84 (1H, brs).

General procedure for the synthesis of LA-18/LA-12/LA-6, 25/26/27

To Amide-Alcohol **21** (1.00 mmol, 328 mg) in 24 mL of dimethylformamide heated to 120 °C under a N_2 atmosphere, was added 224 μL of 1,8-diazabicyclo[5.4.0]undec-7-ene and diphenylphosphoryl azide **24** (1.50 mmol, 323

μL). The reaction was stirred for 2 hours. The reaction mixture was diluted with ether, extracted with water, and brine. The organic layer was subsequently dried over sodium sulfate, filtered and evaporated to dryness. The crude was purified using silica gel column (ethyl acetate:*n*-hexane) to afford:

25/LA-18 as a white solid (112.8 mg, 32% yield). ^{1}H NMR (400MHz; $CDCl_3$) δ (ppm): 0.88 (3H, t, *J* = 6.4 Hz), 1.25-1.29 (28H, m), 1.59-1.65 (2H, m), 2.19 (2H, t, *J* = 7.5 Hz), 3.41-3.48 (4H, m), 5.84 (1H, brs).

26/LA-12 as a white solid (115.4 mg, 43% yield). ^{1}H NMR (400MHz; $CDCl_3$) δ (ppm): 0.88 (3H, t, *J* = 6.4 Hz), 1.26-1.29 (16H, m), 1.60-1.65 (2H, m), 2.19 (2H, t, *J* = 7.5 Hz), 3.40-3.44 (4H, m), 5.79 (1H, brs).

27/LA-6 as a yellow oil (82.9 mg, 45% yield). ^{1}H NMR (400MHz; $CDCl_3$) δ (ppm): 0.90 (3H, t, *J* = 6.6 Hz), 1.27-1.36 (4H, m), 1.60-1.68 (2H, m), 2.20 (2H, t, *J* = 7.4 Hz), 3.40-3.46 (4H, m), 5.88 (1H, brs).

Confocal Microscopic Bacteria Imaging Figure S3:

An overnight bacterial culture was re-grown into fresh medium until 10^8 cells mL^{-1}. After washing with PBS, the bacteria was incubated with **LA-12** (2 μM) for 5 mins at 37 °C. The suspension was subsequently washed with PBS to remove the excess **LA-12**. Following, **DF** (2 μM) staining was carried out for 30 mins at 37 °C before washing of the free **DF** with PBS. The bacteria was then spotted on (3-aminopropyl) triethoxysilane (APTES) pretreated glass slides and covered with coverslips. Labelling of the outer membrane of the bacterial strains were imaged using Zeiss LSM 800 confocal microscope with the excitation at 488 nm.

Confocal Microscopic Bacteria Imaging Figure S4:

An overnight bacterial culture was re-grown into fresh medium until 10^8 cells mL^{-1}. After washing with PBS, the bacteria was incubated with **LA-12** (50 μM) for 1 h at 37 °C. The suspension was subsequently washed with PBS. Following, PI (10 μM) staining was carried out for 15 mins at 37 °C before subjecting to imaging using Zeiss LSM 800 confocal microscope. The bacteria was spotted on APTES pretreated glass slides and covered with coverslips.

Confocal Microscopic Bacteria Imaging Figure S5:

An overnight bacterial culture was re-grown into fresh medium until 10^8 cells mL^{-1}. After washing with PBS, the bacteria was incubated with **LA-12** (50 μM) and AZT inhibitor (100 μM) for 1 h at 37 °C. The suspension was subsequently washed with PBS to remove the excess **LA-12**. Following, **DFD-1** (10 μM) staining was carried out for 30 mins at 37 °C before washing of the free **DFD-1** with PBS. The bacteria was then spotted on APTES pretreated glass slides and covered with coverslips. Inhibition of the Blas enzyme in bacterial strains were imaged using Zeiss LSM 800 confocal microscope.

Minimum Inhibitory Concentration Experiment Table S1:

An overnight bacterial culture was re-grown into fresh medium until 10^8 cells mL^{-1}. The culture is further diluted into 5×10^5 cells mL^{-1} before placing into various test tubes containing different concentration of **DFD-1**. The suspension was incubated for 18 h before the MIC values were determined from OD_{600}, with the OD_{600} value of the culture with absence of bacteria used as the control.

Confocal Microscopic Bacteria Imaging Figure S6:

An overnight bacterial culture was re-grown into fresh medium until 10^8 cells mL^{-1}. After washing with PBS, the bacteria was incubated with **LA-12** (50 μM) for 1 h at 37 °C. The suspension was subsequently washed with PBS to remove the excess **LA-12**. Following, **DF** (10 μM) staining was carried out for 30 mins at 37 °C before washing of the free **DF** with PBS. The bacteria was then spotted on APTES pretreated glass slides and covered with coverslips. The effect of the presence of **LA-12** on the bacterial strains were imaged using Zeiss LSM 800 confocal microscope.

General procedure for the evaluation of click reaction:

An overnight bacterial culture was re-grown into fresh medium until 10^8 cells mL^{-1}. After washing with PBS, the bacteria was incubated with **LA-12** (50 μM) for 1 h at 37 °C. The suspension was subsequently washed with PBS to remove the excess **LA-12**. Following, **DF** (10 μM) staining was carried out for 15 mins at 37 °C before washing of the free **DF** with PBS. The bacteria was then subjected to fluorescence spectrophotometer analysis.

General procedure for the evaluation of enzyme cleavage:

An overnight bacterial culture was re-grown into fresh medium until 10^8 cells mL^{-1}. After washing with PBS, the bacteria was incubated with **LA-12** (50 μM) for 1 h at 37 °C. The suspension was subsequently washed with PBS to remove the excess **LA-12**. Following, **DFD-1** (10 μM) staining was carried out for 15 mins at 37 °C. The bacteria was then subjected directly to fluorescence spectrophotometer analysis.

Flow Cytometry Analysis General Procedure:

An overnight bacterial culture was re-grown into fresh medium until 10^8 cells mL^{-1}. After washing with PBS, the bacteria was incubated with **LA-12** (50 μM) and AZT inhibitor (100 μM) for 1 h at 37 °C. The suspension was subsequently washed with PBS to remove the excess **LA-12**. Following, **DFD-1** (10 μM) staining was carried out for 30 mins at 37 °C before washing of the free **DFD-1** with PBS. The bacteria were then subjected to flow cytometry analysis under the excitation at 488 nm.

3.3 References

1. Llado, S., Lopez-Mondejar, R., Baldrian, P., *Microbiol Mol Biol Rev* **2017,** *81* (2), e00063-16.

2. Cekanaviciute, E., Yoo, B. B., Runia, T. F., Debelius, J. W., Singh, S., Nelson, C. A., Kanner, R., Bencosme, Y., Lee, Y. K., Hauser, S. L., Crabtree-Hartman, E., Sand, I. K., Gacias, M., Zhu, Y., Casaccia, P., Cree, B. A. C., Knight, R., Mazmanian, S. K., Baranzini, S. E., *Proc Natl Acad Sci U S A* **2017,** *114* (40), 10713-10718.

3. Peck, M., Badrick, T., *Journal of Histotechnology* **2017,** *40* (2), 54-61.

4. Boyanova, L., *Postgrad Med* **2018,** *130* (1), 105-110.

5. Jean, N., Bougault, C., Simorre, J. P., GlycoPedia. The Structure of Bacterial Cell Wall. https://glycopedia.eu/The-Bacterial-Cell-Wall (accessed Mar 1, 2018).

6. Nikaido, H., *Microbiol Mol Biol Rev* **2003,** *67* (4), 593-656.

7. Rollauer, S. E., Sooreshjani, M. A., Noinaj, N., Buchanan, S. K., *Philos Trans R Soc Lond B Biol Sci* **2015,** *370* (1679), 20150023.

8. Delcour, A. H., *Biochim Biophys Acta* **2009,** *1794* (5), 808-16.

9. Schwechheimer, C., Kuehn, M. J., *Nat Rev Microbiol* **2015,** *13*, 605.

10. Squeglia, F., Ruggiero, A., Berisio, R., *Chemistry* **2018,** *24* (11), 2533-2546.

11. Mattei, P. J., Neves, D., Dessen, A., *Curr Opin Struct Biol* **2010,** *20* (6), 749-55.

12. Labischinski, H., Goodell, E. W., Goodell, A., Hochberg, M. L., *J Bacteriol* **1991,** *173* (2), 751-6.

13. Vollmer, W., Seligman, S. J., *Trends Microbiol* **2010,** *18* (2), 59-66.

14. Beeby, M., Gumbart, J. C., Roux, B., Jensen, G. J., *Mol Microbiol* **2013,** *88* (4), 664-72.

15. Cordillot, M., Dubee, V., Triboulet, S., Dubost, L., Marie, A., Hugonnet, J. E., Arthur, M., Mainardi, J. L., *Antimicrob Agents Chemother* **2013,** *57* (12), 5940-5.

16. Aminov, R., *Biochem Pharmacol* **2017,** *133*, 4-19.

17. Kong, K. F., Schneper, L., Mathee, K., *APMIS* **2010,** *118* (1), 1-36.

18. Zeng, X., Lin, J., *Front Microbiol* **2013,** *4*, 128.

19. Kuzin, A. P., Sun, T., Jorczak-Baillass, J., Healy, V. L., Walsh, C. T., Knox, J. R., *Structure* **2000,** *8* (5), 463-470.

20. Healy, V. L., Lessard, I. A. D., Roper, D. I., Knox, J. R., Walsh, C. T., *Chemistry & Biology* **2000,** *7* (5), R109-R119.

21. Nicola, G., Tomberg, J., Pratt, R. F., Nicholas, R. A., Davies, C., *Biochemistry* **2010,** *49* (37), 8094-104.

22. Curley, K., Pratt, R. F., *Bioorg Chem* **2000,** *28* (6), 338-56.

23. Murphy, B. P., Pratt, R. F., *Biochem J* **1988,** *256* (2), 669-72.

24. Sarma, S. C., SlideShare. Beta Lactam Antibiotics. https://www.slideshare.net/saurav9119/beta-lactam-antibiotics-43630735 (accessed 8 Mar 2018).

25. Aminov, R. I., *Front Microbiol* **2010,** *1*, 134.

26. Fleming, A., *Br. J. Exp. Pathol.* **1929,** *10*, 226-236.

27. Lewis, K., *Nature* **2012,** *485*, 439.

28. Shephard, R. J., In *A History of Health & Fitness: Implications for Policy Today.* Springer, Cham, **2018**, 381-393.

29. Shama, G., *J. Pharm. Microbiol.* **2017,** *3* (1).

30. Burdon-Sanderson, *Quarterly Journal of Microscopical Science* **1871,** *s2-11* (44), 323-352.

31. Roberts, W., *Philos Trans R Soc Lond.* **1874,** *164*, 457-77.

32. Lister, J., *Trans R Soc Edinburg.* **1875,** *27*, 313.

33. Tyndall, J., *Br Med J* **1876,** *1* (787), 121-4.

34. Pasteur, L., Joubert, J. F., *C. R. Acad. Sci. Paris.* **1877,** *85*, 101-15.

35. Newton, G. G., Abraham, E. P., *Biochem J* **1956,** *62* (4), 651-8.

36. Abraham, E. P., Newton, G. G., *Biochem J* **1954,** *58* (1), 94-102.

37. Parker, W. L., Cimarusti, C. M., Floyd, D. M., Koster, W. H., Liu, W. C., *J Antimicrob Chemother* **1981,** *8 Suppl E*, 17-20.

38. Kahan, J. S., Kahan, F. M., Goegelman, R., Currie, S. A., Jackson, M., Stapley, E. O., Miller, T. W., Miller, A. K., Hendlin, D., Mochales, S., Hernandez, S., Woodruff, H. B., Birnbaum, J., *J Antibiot (Tokyo)* **1979,** *32* (1), 1-12.

39. Watkins, R. R., Bonomo, R. A., In *Infectious Diseases (Fourth Edition)*, Elsevier, **2017**, Vol. 2, 1203-1216.e2.

40. McKinnon, P. S., Paladino, J. A., Schentag, J. J., *Int J Antimicrob Agents* **2008,** *31* (4), 345-351.

41. Craig, W. A., *Clin Infect Dis* **2001,** *33* (Supplement_3), S233-S237.

42. Finberg, R. W., Guharoy, R., In *Clinical Use of Anti-infective Agents*, Springer Science+Business Media, LLC, **2012**, 5-14.

43. Bradley, J. S., Sauberan, J. B., In *Principles and Practice of Pediatric Infectious Diseases (Fourth Edition)*, Elsevier: London, **2012**, 1453-1484.e5.

44. Castle, S. S., In *xPharm: The Comprehensive Pharmacology Reference*, Elsevier: New York, **2007,** 1-3.

45. Farrington, M., In *Clinical Pharmacology (Eleventh Edition)*, Churchill Livingstone: Oxford, **2012,** 173-190.

46. Maddison, J. E., Watson, A. D. J., Elliott, J., In *Small Animal Clinical Pharmacology (Second Edition)*, Saunders: Edinburgh, **2008,** 148-185.

47. Hubschwerlen, C., In *Comprehensive Medicinal Chemistry II*, Elsevier: Oxford, **2007,** 479-518.

48. Garbis, H., van Tonningen, M. R., Reuvers, M., In *Drugs During Pregnancy and Lactation (Second Edition)*, Academic Press: Oxford, **2007,** 123-177.

49. Scholar, E., In *xPharm: The Comprehensive Pharmacology Reference*, Elsevier: New York, **2007,** 1-4.

50. Wetzel, S., Lachance, H., Waldmann, H., In *Comprehensive Natural Products II*, Elsevier: Oxford, **2010,** 5-46.

51. Kuriyama, T., Karasawa, T., Williams, D. W., In *Biofilms in Infection Prevention and Control*, Academic Press: Boston, **2014,** 209-244.

52. Brook, I., In *Infectious Diseases (Fourth Edition)*, Elsevier, **2017,** 1628-1644.e2.

53. Ballal, M., In *Antibiotic Resistance*, Academic Press: 2016, 63-92.

54. Davies, J., Davies, D., *Microbiol Mol Biol Rev* **2010,** *74* (3), 417-33.

55. Mizukami, S., Watanabe, S., Hori, Y., Kikuchi, K., *J Am Chem Soc* **2009,** *131* (14), 5016-7.

56. Guillaume, G., Vanhove, M., Lamotte-Brasseur, J., Ledent, P., Jamin, M., Joris, B., Frere, J. M., *J Biol Chem* **1997,** *272* (9), 5438-44.

57. Gao, W., Xing, B., Tsien, R. Y., Rao, J., *J Am Chem Soc* **2003,** *125* (37), 11146-7.

58. Bush, K., Jacoby, G. A., *Antimicrob Agents Chemother* **2010,** *54* (3), 969-76.

59. Hall, B. G., Barlow, M., *Journal of Antimicrobial Chemotherapy* **2005,** *55* (6), 1050-1051.

60. Bush, K., Jacoby, G., *J Antimicrob Chemother* **1997,** *39* (1), 1-3.

61. Thomson, K. S., Smith Moland, E., *Microbes and Infection* **2000,** *2* (10), 1225-1235.

62. Thomson, K. S., *J Clin Microbiol* **2010,** *48* (4), 1019-25.

63. Pasteran, F., Mendez, T., Guerriero, L., Rapoport, M., Corso, A., *J Clin Microbiol* **2009,** *47* (6), 1631-9.

64. Xie, H., Mire, J., Kong, Y., Chang, M., Hassounah, H. A., Thornton, C. N., Sacchettini, J. C., Cirillo, J. D., Rao, J., *Nat Chem* **2012,** *4* (10), 802-9.

65. Aw, J., Widjaja, F., Ding, Y., Mu, J., Liang, Y., Xing, B., *Chem Commun (Camb)* **2017,** *53* (23), 3330-3333.

66. Papp-Wallace, K. M., Endimiani, A., Taracila, M. A., Bonomo, R. A., *Antimicrob Agents Chemother* **2011,** *55* (11), 4943-60.

67. Bebrone, C., *Biochemical Pharmacology* **2007,** *74* (12), 1686-1701.

68. Hall, B. G., Salipante, S. J., Barlow, M., *J Mol Evol* **2003,** *57* (3), 249-54.

69. Palzkill, T., *Ann N Y Acad Sci* **2013,** *1277*, 91-104.

70. Jacoby, G. A., *Clin Microbiol Rev* **2009,** *22* (1), 161-82.

71. Perez-Perez, F. J., Hanson, N. D., *J Clin Microbiol* **2002,** *40* (6), 2153-62.

72. Liebana, E., Carattoli, A., Coque, T. M., Hasman, H., Magiorakos, A. P., Mevius, D., Peixe, L., Poirel, L., Schuepbach-Regula, G., Torneke, K., Torren-Edo, J., Torres, C., Threlfall, J., *Clin Infect Dis* **2013,** *56* (7), 1030-7.

73. Doi, Y., Paterson, D. L., *Int J Infect Dis* **2007,** *11* (3), 191-7.

74. Coudron, P. E., Moland, E. S., Thomson, K. S., *J Clin Microbiol* **2000,** *38* (5), 1791-6.

75. Tamma, P. D., Girdwood, S. C., Gopaul, R., Tekle, T., Roberts, A. A., Harris, A. D., Cosgrove, S. E., Carroll, K. C., *Clin Infect Dis* **2013,** *57* (6), 781-8.

76. Philippon, A., Arlet, G., Jacoby, G. A., *Antimicrob Agents Chemother* **2002,** *46* (1), 1-11.

77. Pai, H., Kang, C. I., Byeon, J. H., Lee, K. D., Park, W. B., Kim, H. B., Kim, E. C., Oh, M. D., Choe, K. W., *Antimicrob Agents Chemother* **2004,** *48* (10), 3720-8.

78. Sanders, W. E., Jr., Sanders, C. C., *Clin Microbiol Rev* **1997,** *10* (2), 220-41.

79. Chen, J., Shang, X., Hu, F., Lao, X., Gao, X., Zheng, H., Yao, W., *Mini-Reviews in Medicinal Chemistry* **2013,** *13* (13), 1846-1861.

80. Shaya, J., Collot, M., Bénailly, F., Mahmoud, N., Mély, Y., Michel, B. Y., Klymchenko, A. S., Burger, A., *ACS Chemical Biology* **2017,** *12* (12), 3022-3030.

81. Thorn, K., *Mol Biol Cell* **2016,** *27* (2), 219-22.

82. Qian, L., Li, L., Yao, S. Q., *Acc Chem Res* **2016,** *49* (4), 626-34.

83. Dong, B., Song, X., Wang, C., Kong, X., Tang, Y., Lin, W., *Analytical Chemistry* **2016,** *88* (7), 4085-4091.

84. Demchenko, A. P., In *Introduction to Fluorescence Sensing, 2nd ed,* Springer: Switzerland, **2015,** 359-416.

85. Shao, Q., Zheng, Y., Dong, X., Tang, K., Yan, X., Xing, B., *Chem Eur J* **2013,** *19* (33), 10903-10.

86. Li, L., Li, Z., Shi, W., Li, X., Ma, H., *Anal Chem* **2014,** *86* (12), 6115-20.

87. Mao, W., Xia, L., Wang, Y., Xie, H., *Chem Asian J* **2016,** *11* (24), 3493-3497.

88. Zhang, J., Chen, Y. P., Miller, K. P., Ganewatta, M. S., Bam, M., Yan, Y., Nagarkatti, M., Decho, A. W., Tang, C., *J Am Chem Soc* **2014,** *136* (13), 4873-6.

89. Yang, Y., Rasmussen, B. A., Shlaes, D. M., *Pharmacol Ther* **1999,** *83* (2), 141-51.

90. Nukaga, M., Mayama, K., Hujer, A. M., Bonomo, R. A., Knox, J. R., *J Mol Biol* **2003,** *328* (1), 289-301.

91. Harris, P. N., Ferguson, J. K., *Int J Antimicrob Agents* **2012,** *40* (4), 297-305.

92. Negri, M. C., Baquero, F., *Clin Microbiol Infect* **1998,** *4* (10), 585-588.

93. Braine, T., *Bull World Health Organ* **2011,** *89* (2), 88-9.

94. Mizukami, S., Hori, Y., Kikuchi, K., *Acc Chem Res* **2014,** *47* (1), 247-56.

95. Shao, Q., Xing, B., *Chem Commun (Camb)* **2012,** *48* (12), 1739-41.

96. Xing, B., Khanamiryan, A., Rao, J., *J Am Chem Soc* **2005,** *127* (12), 4158-9.

97. Lobkovsky, E., Moews, P. C., Liu, H., Zhao, H., Frere, J. M., Knox, J. R., *Proc Natl Acad Sci U S A* **1993,** *90* (23), 11257-61.

98. King, D., Strynadka, N., *Protein Sci* **2011,** *20* (9), 1484-91.

99. Lahiri, S. D., Johnstone, M. R., Ross, P. L., McLaughlin, R. E., Olivier, N. B., Alm, R. A., *Antimicrob Agents Chemother* **2014,** *58* (10), 5704-13.

100. Fisher, J. F., Meroueh, S. O., Mobashery, S., *Chem Rev* **2005,** *105* (2), 395-424.

101. Kahne, D., Leimkuhler, C., Lu, W., Walsh, C., *Chem Rev* **2005,** *105* (2), 425-48.

102. Lim, D., Strynadka, N. C. J., *Nature Structural Biology* **2002,** *9*, 870.

103. Sauvage, E., Kerff, F., Terrak, M., Ayala, J. A., Charlier, P., *FEMS Microbiol Rev* **2008,** *32* (2), 234-58.

104. Alekshun, M. N., Levy, S. B., *Cell* **2007,** *128* (6), 1037-50.

105. Bebrone, C., Lassaux, P., Vercheval, L., Sohier, J. S., Jehaes, A., Sauvage, E., Galleni, M., *Drugs* **2010,** *70* (6), 651-79.

106. Drawz, S. M., Bonomo, R. A., *Clin Microbiol Rev* **2010,** *23* (1), 160-201.

107. Zhang, J., Shen, Y., May, S. L., Nelson, D. C., Li, S., *Angew Chem Int Ed Engl* **2012,** *51* (8), 1865-8.

108. Hart, K. M., Reck, M., Bowman, G. R., Wencewicz, T. A., *MedChemComm* **2016,** *7* (1), 118-127.

109. Yang, Z., Ho, P. L., Liang, G., Chow, K. H., Wang, Q., Cao, Y., Guo, Z., Xu, B., *J Am Chem Soc* **2007,** *129* (2), 266-7.

110. Staub, I., Sieber, S. A., *J Am Chem Soc* **2008,** *130* (40), 13400-9.

111. Moya, B., Dotsch, A., Juan, C., Blazquez, J., Zamorano, L., Haussler, S., Oliver, A., *PLoS Pathog* **2009,** *5* (3), e1000353.

112. Roy, R., Hohng, S., Ha, T., *Nat Methods* **2008,** *5* (6), 507-16.

113. Lovell, J. F., Liu, T. W., Chen, J., Zheng, G., *Chem Rev* **2010,** *110* (5), 2839-57.

114. Bandyopadhyay, A., McCarthy, K. A., Kelly, M. A., Gao, J., *Nat Commun* **2015,** *6*, 6561.

115. Liang, H., DeMeester, K. E., Hou, C. W., Parent, M. A., Caplan, J. L., Grimes, C. L., *Nat Commun* **2017,** *8*, 15015.

116. Lingwood, D., Simons, K., *Science* **2010,** *327* (5961), 46-50.

117. Phillips, R., Ursell, T., Wiggins, P., Sens, P., *Nature* **2009,** *459* (7245), 379-85.

118. Fosso, M. Y., Shrestha, S. K., Green, K. D., Garneau-Tsodikova, S., *J Med Chem* **2015,** *58* (23), 9124-32.

119. Lyu, S. Y., Liu, Y. C., Chang, C. Y., Huang, C. J., Chiu, Y. H., Huang, C. M., Hsu, N. S., Lin, K. H., Wu, C. J., Tsai, M. D., Li, T. L., *J Am Chem Soc* **2014,** *136* (31), 10989-95.

120. Benhamou, R. I., Shaul, P., Herzog, I. M., Fridman, M., *Angew Chem Int Ed Engl* **2015,** *54* (46), 13617-21.

121. Benhamou, R. I., Bibi, M., Steinbuch, K. B., Engel, H., Levin, M., Roichman, Y., Berman, J., Fridman, M., *ACS Chem Biol* **2017,** *12* (7), 1769-1777.

122. Fan, Q., Cheng, K., Hu, X., Ma, X., Zhang, R., Yang, M., Lu, X., Xing, L., Huang, W., Gambhir, S. S., Cheng, Z., *J Am Chem Soc* **2014,** *136* (43), 15185-94.

123. Mu, J., Liu, F., Rajab, M. S., Shi, M., Li, S., Goh, C., Lu, L., Xu, Q. H., Liu, B., Ng, L. G., Xing, B., *Angew Chem Int Ed Engl* **2014,** *53* (52), 14357-62.

124. Cobos-Correa, A., Trojanek, J. B., Diemer, S., Mall, M. A., Schultz, C., *Nat Chem Biol* **2009,** *5* (9), 628-30.

125. Oshikawa, Y., Furuta, K., Tanaka, S., Ojida, A., *Anal Chem* **2016,** *88* (3), 1526-9.

126. Yarlagadda, V., Akkapeddi, P., Manjunath, G. B., Haldar, J., *J Med Chem* **2014,** *57* (11), 4558-68.

127. Sautrey, G., Zimmermann, L., Deleu, M., Delbar, A., Souza Machado, L., Jeannot, K., Van Bambeke, F., Buyck, J. M., Decout, J. L., Mingeot-Leclercq, M. P., *Antimicrob Agents Chemother* **2014,** *58* (8), 4420-30.

128. Morita, Y., Tomida, J., Kawamura, Y., *Front Microbiol* **2014,** *4*, 422.

129. Stover, C. K., Pham, X. Q., Erwin, A. L., Mizoguchi, S. D., Warrener, P., Hickey, M. J., Brinkman, F. S., Hufnagle, W. O., Kowalik, D. J., Lagrou, M., Garber,

R. L., Goltry, L., Tolentino, E., Westbrock-Wadman, S., Yuan, Y., Brody, L. L., Coulter, S. N., Folger, K. R., Kas, A., Larbig, K., Lim, R., Smith, K., Spencer, D., Wong, G. K., Wu, Z., Paulsen, I. T., Reizer, J., Saier, M. H., Hancock, R. E., Lory, S., Olson, M. V., *Nature* **2000,** *406* (6799), 959-64.

130. Smith, J. R., Barber, K. E., Raut, A., Aboutaleb, M., Sakoulas, G., Rybak, M. J., *J Antimicrob Chemother* **2015,** *70* (6), 1738-43.

131. Sakoulas, G., Bayer, A. S., Pogliano, J., Tsuji, B. T., Yang, S. J., Mishra, N. N., Nizet, V., Yeaman, M. R., Moise, P. A., *Antimicrob Agents Chemother* **2012,** *56* (2), 838-44.

132. Morandi, F., Caselli, E., Morandi, S., Focia, P. J., Blázquez, J., Shoichet, B. K., Prati, F., *J Am Chem Soc* **2003,** *125* (3), 685-95.